Potential of Vehicle-to-Grid Ancillary Services Considering the Uncertainties in Plug-in Electric Vehicle Availability and Service/Localization Limitations in Distribution Grids

Siyamak Sarabi, Arnaud Davigny, Vincent Courtecuisse, Yann Riffonneau, Benoit Robyns

PREPRINT

Potential of Vehicle-to-Grid Ancillary Services Considering the Uncertainties in Plug-in Electric Vehicle Availability and Service/Localization Limitations in Distribution Grids

Siyamak Sarabi[a,b,c,*], Arnaud Davigny[a,b], Vincent Courtecuisse[d], Yann Riffonneau[e], Benoît Robyns[a,b]

[a] *Univ. Lille, EA 2697 - L2EP - Lille Laboratory of Electrical Engineering and Power Electronics, F-59000 Lille, France*
[b] *School of High Studies for Engineering (HEI) - 13, rue de Toul, BP 41290, 59014 Lille cedex, France*
[c] *ADEME, French Environment and Energy Management Agency - 20, avenue du Grésillé BP 90406, 49004 Angers, France*
[d] *GEREDIS Deux-Sèvres, Deux-Sèvres departement Distribution System Operator (DSO) - 18 Rue Joule, 79000 Niort, France*
[e] *SNCF, Innovation and Research - 40 avenue des Terroirs de France, 75611 Paris, France*

Abstract

The aim of the paper is to propose an approach for statistical assessment of the potential of plug-in electric vehicles (PEV) for vehicle-to-grid (V2G) ancillary services, where it focuses on PEVs doing daily home-work commuting. In this approach, the possible ancillary services (A/S) for each PEV fleet in terms of its available V2G power (AVP) and flexible intervals are identified. The flexible interval is calculated using a powerful stochastic global optimization technique so-called "Free Pattern Search" (FPS). A probabilistic method is also proposed to quantify the impacts of PEV's availability uncertainty using the Gaussian mixture model (GMM), and interdependency of stochastic variables on AVP of each fleet thanks to a multivariate modeling with Copula function. Each fleet is analyzed based on its aggregated PEV numbers at different level of distribution grid, in order to satisfy the ancillary services localization limitation. A case study using the proposed approach evaluates the real potential in Niort, a city in west of France. In fact, by using the proposed approach an aggregator can analyze the V2G potential of PEVs under its contract.

Keywords: Vehicle-to-grid, Ancillary services, Distribution grid, Gaussian Mixture model, Copula function, Free Pattern Search

1. Introduction

Massive production perspective of plug-in electric vehicles (PEVs) causes serious challenges and grid congestion for the utility grids. The researches have shown that electricity distribution grid can be highly affected by arbitrary charging demand of electric vehicles [1–3]. However, vehicle-to-grid (V2G) technology and charging coordination during off-peak hours of local distribution grids have been proposed as solutions [4–7]. In addition, V2G enabled PEVs, which have the ability to inject power to the grid, have been presented as grid supporters [8] and potential ancillary service (A/S) providers, where eventually make the transportation electrification beneficial for the grids [9].

Nomenclature

PEV	Plug-in Electric Vehicle
V2G	Vehicle-to-Grid
G2V	Grid-to-Vehicle
A/S	Ancillary Service
AVP	Available V2G Power
FPS	Free Pattern Search
GMM	Gaussian Mixture Model
HV	High Voltage
MV	Medium Voltage
LV	Low Voltage
TSO	Transmission System Operator
DSO	Distribution System Operator
SOC	State Of Charge
pdf	probability distribution function
FIS	Fuzzy Inference System
NEDC	New European Driving Cycle
DoD	Depth of Discharge
BC1	Bidding Capacity 1
BC2	Bidding Capacity 2
BC3	Bidding Capacity 3
MLE	Maximum Likelihood Estimation
MCS	Monte Carlo Simulation
RF	Reliability Factor
BS	Bidding Start time
HJPS	Hooke and Jeeves Pattern Search
FS	Free Search
DLP	Daily Load Profile
BM	Balancing Mechanism
PPSMV	Peak Power Shaving - Medium Voltage
PPSLV	Peak Power Shaving - Low Voltage
VRMV	Voltage Regulation - Medium Voltage
VRLV	Voltage Regulation - Low Voltage
LM	Losses Minimization
ETCM	Energy Transmission Cost Minimization
FR	Frequency Regulation
DUR	Duration, input for Fuzzy system

In the literature, the economic [10–13] and technical [14, 15] feasibilities of PEV fleet as the energy storage and service providers are discussed. They are considered in different services markets such as, regulation, spinning reserve [16], peak power support [17] and power quality [18] and more from economic point of view. While, technical analyses are mainly limited to capacity estimation, optimal coordination, aggregator communication architectures and battery degradation impacts [15, 17, 19, 20]. The points related to aggregator volume requirements, grid/services localization limitations and PEVs availability uncertainty impacts on bidding capacities are not discussed or less explored. In addition, the aggregator volume in terms of the required number of vehicles for providing each ancillary service is not analyzed up to now.

*Corresponding author
Email address: siyamak.sarabi@hei.fr (Siyamak Sarabi)

In term of the energy management systems for plug-in electric vehicles and V2G technologies, different scheduling and management schemes are developed. An adaptive intelligent system using fuzzy logic controller and adaptive neuro-fuzzy inference system (ANFIS) is developed in [21]. In [22] an intelligent energy management using cloud computing network is proposed. These technics reduce operation of electric vehicle, grid and parking lot as well as the load demand prediction. A large scale fuzzy logic based intelligent control for V2G is also proposed in [23] which provides different services such as, peak power, balancing control, load levelling and voltage regulation. For specific services, different control strategies are developed. For instance, a preventive control strategy for controlling static voltage stability is proposed in [24, 25] which maintains the static voltage stability of power system under the V2G concept and evaluates the V2G response capability with different charging strategies during a whole day.

The innovative aspects of this paper compared to the aforementioned papers is considering the uncertainty impact on the V2G capacity, and scalability of the flexible V2G power capacity for different level of distribution grid by considering localization limitation of different services. Hence the service assessment can be applicable up to the low voltage (LV) distribution grid services such as voltage regulation and load levelling at LV grid. Interdependency of stochastic variables such as arrival time, departure time and driving distance are also modelled and their impacts on the contracted power are analyzed.

The novelty of the paper is that it has provided a multi-level methodological approach in order to assess the V2G potential, suitable for regional distribution system operators. In this approach, the PEVs' availability uncertainty and localization/limitation are considered as the main factors affecting the potential of V2G for grid ancillary service participation. A probabilistic model is developed in order to estimate the availability uncertainty using only daily trips probability data. The interdependency of the stochastic variables are also modeled using a copula function. This modeling approach, takes into account the impact of uncertainty on the bidding capacities and improve the reliability of the contracted bidding. In addition, in order to be realistic, the distribution of electric vehicles in the distribution grid is estimated using real customers' distribution data to estimate the real potential of PEV fleet for different ancillary services.

A/S providers at the distribution grid level are faced with the localization limitation for each type of service. Such limitations make difficult to achieve the services' requirements for PEV aggregators, as the aggregated number of PEVs at the different level of the grid is not always sufficient. Moreover, the aggregators need to have sufficient information for offering a reliable bidding capacity, which depend upon the type of services for which they would be the candidate. However, the general requirements are the amount of energy in form of power and time interval. These are predefined by grid actors based on the grid characteristics in different countries[1]. The constraints related to PEVs aggregation such as, available aggregated power and PEVs availability uncertainty should be taken into account in order to be competitive in the markets. These

[1]From August 2014, RTE, the French transmission system operator (TSO), announced that industrial consumers henceforth could be reserve service providers with a minimum power of 2 MW [26]. This is also estimated for the distributed energy storage systems at the distribution grid level with a minimum of 1 to 2 MW power [27].

constraints are the main concerns of this paper, where the effort is to propose an approach for potential assessment of a candidate PEV fleet under an aggregation contract, particularly at the level of distribution grid by considering; **1)** Available V2G power of the fleet, **2)** Availability uncertainty of the fleet and its impacts on the bidding capacities' reliability, **3)** The flexibility of the available power interval under bidding capacity contracts and **4)** Distribution grid services/localization limitations.

In this paper, at first the general approach for ancillary service assessment of V2G enabled PEVs at the distribution grid level is introduced. Afterwards, all necessary input data for the assessment are identified. The methodology is applied on Niort, a city in west of France, considering its mobility statistics and distribution grid topology. The methodologies for available V2G power modeling, availability uncertainty modeling, the flexibility of the bidding capacities' calculation and the service assessment system will be explained thoroughly in the next sections. A general research background is presented to show actual solutions and the main contribution of paper for V2G ancillary service assessment.

2. Research background

Different methods have been proposed for capacity estimation of PEV fleet, but none of them consider the localization limitation of the services. Reference [15] calculates achievable power capacity by binomial distribution of clustered PEVs. Reference [28] uses the survey data to identify the location of PEVs during the day. In [29] Monte Carlo simulation is used to estimate the probability of transition between different states, e.g. parked or movement for different parking location. A non-homogeneous semi-Markov process is used in [30] for PEV availability and identifying the charging load, while in [31] a continuous time non-Markov chain is chosen as the mobility patterns do not fulfill the Markov property (memorylessness). Reference [32] uses the trip chains for mobility modeling of PEV fleet and concluded that the home and office car parks have maximum availability among other place parkings. Among all of these researches backgrounds and our case study mobility survey, we concluded that the PEVs are parked in home and office parkings mostly a day and their service providing potential at these time intervals is relatively higher than other places, such as parking lots of shopping centers or the streets, which are highly stochastic and periodically short.

The second limitation is the uncertainties associated with availability of the PEVs for service providing. Reference [33] defines the uncertainty sources as the model based uncertainties and forecasting based uncertainties. The model-based uncertainties come from the aggregated battery model instead of the individual battery model [2]. The second source is related to forecasting data such as arrival, departure time, driving behavior and arrival state of charge (SOC) of PEVs. In [34], the driving behavior uncertainty is modeled with individual driving behavior with the non-Markov chain process by the states' transition probabilities defined based on mobility survey data. In [35], a two-state single node Monte Carlo simulation is used to represent the uncertainty in driving behavior by concentrating on stochastic variables with the independent

[2] In modeling large number of PEVs it would be impractical to model all batteries' dynamics in detail.

sampling process. While in this paper, interdependency of stochastic variables are modeled in a multivariate manner using copula function.

The predictable sources of uncertainties are normally following a particular probability distribution. These are known as arrival time, departure time and driving distance distribution. In addition, in the future smart grid, the communication infrastructures will facilitate accessibility and predictability of such information. Therefore, considering highly enough accurate prediction system, the uncertainties associated with prediction errors can be negligible. In the other side, there are some sources of uncertainty, which are not predictable at all, like the unforeseen departure of PEVs during their stationing time (plug-in time). Considering that, a probabilistic approach is proposed for this study, that can provide the probability distribution function (pdf) of availability uncertainty. The advantage with this approach is the ability to quantify the availability uncertainty impact on the bidding capacities by only knowing the daily trips percentage, arrival and departure time probability of the fleet.

3. General Approach

The general approach consists of 6 sub-blocks, each doing a particular task for the final objective (Fig. 1):

Available V2G power modeling (AVPM) is designed to model the available V2G power for PEVs arriving at office in the morning and PEVS arriving at home in the afternoon. Fundamental parameters for modeling the available V2G power are calculated in **Fundamental parameters estimation FPE** block, which contain arrival SOC, V2G energy, G2V energy and plug-in interval. These parameters which are the indirect parameters will be calculated using the output parameters of MMSV block and averaged PEV characteristic parameters such as, driving efficiency, charging, discharging efficiency, NEDC autonomy and averaged battery capacity of the fleet. In **Multivariate modeling of stochastic variables (MMSV)** block, correlation between arrival time, departure time and driving distance is explored for PEVs doing daily home-work commuting using copula function. This issue is considered as one of the possible uncertainty on the contracted V2G power. A novel approach is proposed in **Probabilistic availability uncertainty modeling (PAUM)** block, which uses only the daily trips percentage data in order to associate a probability density function to the availability uncertainty phenomena. Afterwards, the flexibility of each bidding capacity will be calculated in **Bidding flexibility calculation (BFC)** block using a global stochastic optimization method so-called "Free Pattern Search", which is chosen for its robustness and convergence quality for high dimension stochastic problems. Finally, in **Fuzzy inference system service assessment (FISSA)** block, a fuzzy inference system (FIS) is designed for service assessment of each PEV fleet based on the PEVs population provision of the city under study. This system uses the AVP of each bidding and its flexibility as FIS inputs and will generate a potential factor of 0 to 1 in order to evaluate the fleet potential for each service. In addition, a grid service/localization limit factor is considered to evaluate the aggregated number of PEVs at the appropriate location of the grid.

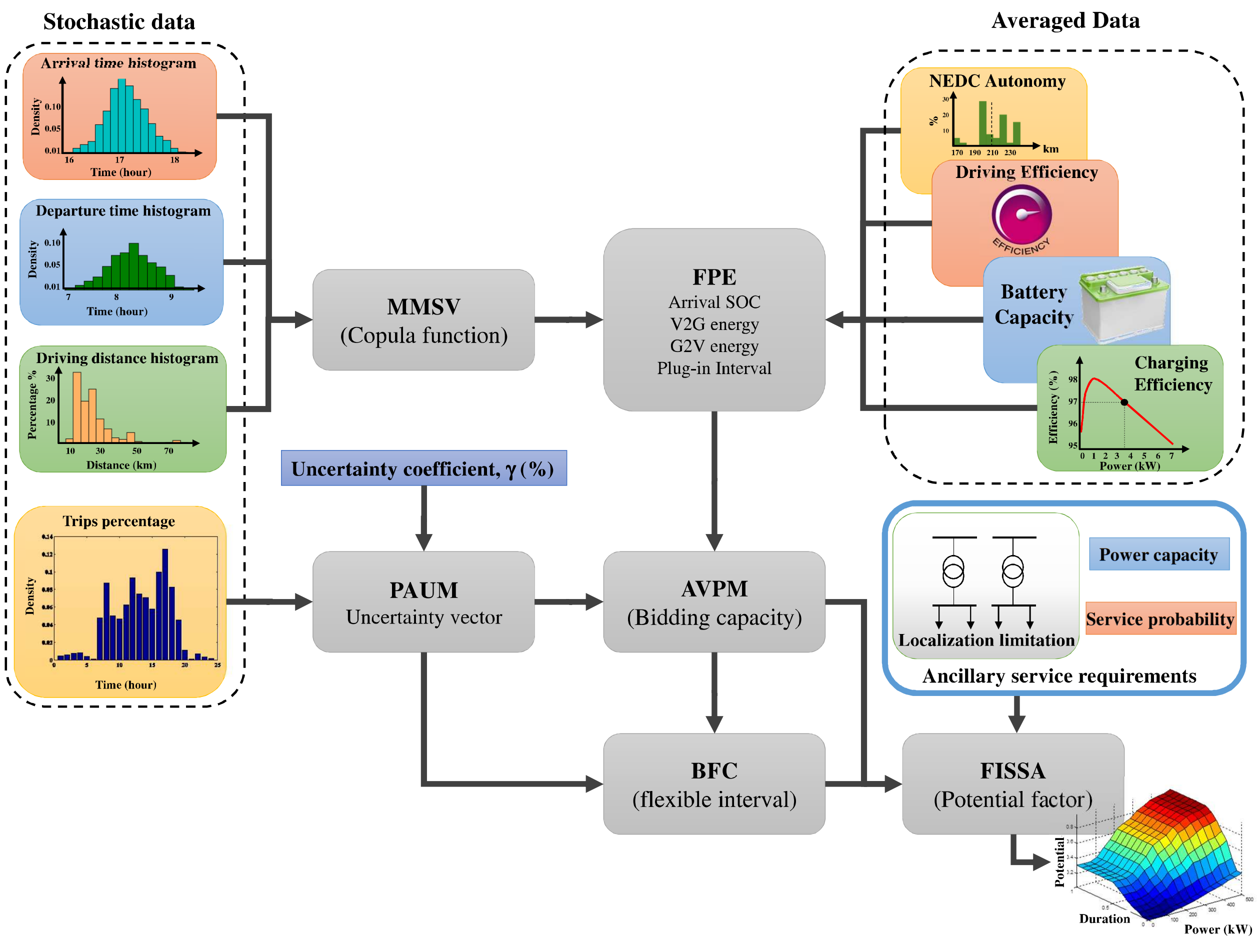

Fig. 1: General framework of V2G ancillary service assessment approach.

4. Case study and Input data

It is assumed, the statistical information about the place under study is available, where the approach will be applicable when the data can be available via the smart grid communication. This approach is practical for local DSO, managing the middle cities' grid operations. The statistical data of Niort city in France are considered as case study [36]. The two evolution scenarios of EVs in France up to 2030 are considered in this study [37, 38] (Table 1). Having the vehicle fleet statistics of Niort and its population, the PEV evolution can be calculated for this city. The cars-per-capita quota is used in order to transfer the unit from population to the car number [39]. The PEV case study scenarios are brought in Table. 2.

Table 1: PEV evolution scenarios in France (PEV numbers in Million).

Evolution horizon	2013	2015	2020	2025	2030
Low Scenario	0.042	0.05	0.8	1.7	2.5
High Scenario	0.05	0.3	0.2	5.5	9

Table 2: PEV evolution scenarios for Niort city.

Evolution horizon	2020	2025	2030
Low Scenario (PEV number)	851	1808	2659
High Scenario (PEV number)	2127	5849	9572

The input data are divided in two main natures; averaged data and stochastic data. Averaged data are containing the vehicle characteristics, which help to estimate the available and consumed energy of the vehicle's battery. For this study, based on the actual French electric vehicles market, the values are considered as in Table. 3. The stochastic variables sampled from statistical survey are; **Arrival time distribution**, **Departure time distribution**, **Daily Driving distance distribution** and **Daily trips percentage**.

Table 3: Averaged PEV characteristics in French market.

Parameter	**Symbol**	**Value**
Battery Capacity	E_{ev}	22 kWh
Charging/Discharging efficiency	η_{cd}	97.5%
Charging/Discharging power	P_{ch}	3.7 kW
NEDC autonomy	A	210 km
Driving efficiency	η_{ev}	97% (9.2 km/kWh)
Admissible depth of discharge	DoD	80%

The arrival and departure time's distribution of both home and office scenario are following approximately a Gaussian distribution with the parameters as follows; Home departure (μ=07h45), Home arrival (μ=17h15), Office Arrival (μ=08h15), Office departure (μ=16h45), Home-work trips (μ=08h00) and Work-home trips (μ=17h00) and the σ=30 min for all cases. The daily driving distance distribution of home scenario takes into account a daily round trip and for office scenario, a single way trip to the office and both are approximated to follow the same distribution (Fig. 2).

Daily trips percentage data show the hourly percentage of the trips for a working day done by personal vehicles for the Niort city. This distribution is used in order to model the availability uncertainty of the PEVs (Fig. 3).

5. Available V2G power modeling (AVPM)

In this study, AVP of home-work commuting PEV fleet has been evaluated in two potential intervals. First V2G at work only and second V2G at home only. The main assumptions behind the work are as follows:

- Charging/discharging rate at normal level (16A, 230 V, 3.7 kW).
- The PEV will provide V2G service once in a day and will be fully charged once in a day.

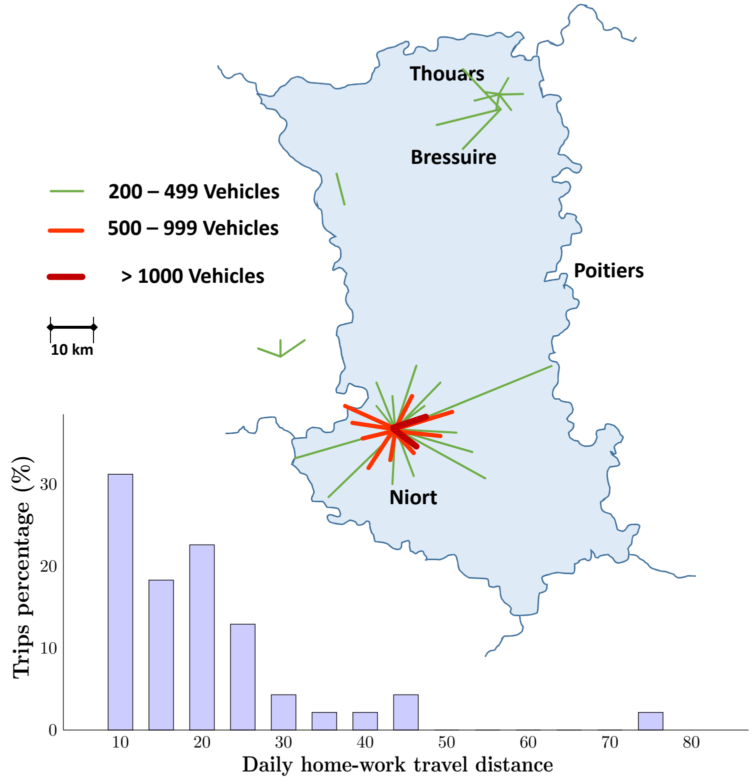

Fig. 2: Daily driving distance for home-work commuting in Niort [36].

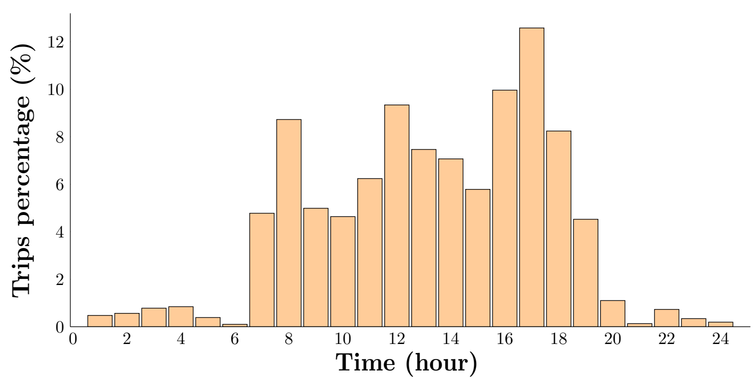

Fig. 3: Daily trips percentage in Niort city [40].

- 2 scenarios for V2G service assessment have been considered:
  - V2G at home (the PEV will make a round trip and then provide V2G at home only).
  - V2G at work (the PEV after arrival to the office will provide V2G at work, considering energy need for its return and minimum energy of 20% as constraint to reduce the degradation impact of V2G, i.e. 80% Depth of Discharge (DoD)).

For home scenario, PEVs will be fully charged at departure time, while at the office scenario, PEVs have sufficient energy for the return trip plus 20% energy in battery. These assumptions were made to evaluate the maximum possible potential for aggregated V2G power during each interval. The fact is that, if we consider that PEVs will provide V2G services both at home and office, leading to portioned aggregated V2G power between home and office intervals.

5.1. Fundamental parameter estimation (FPE)

AVP modeling flowchart is provided in Fig. 4. Availability of each PEV in the V2G enabled parking, and its stored battery energy at arrival time are the key information in defining the AVP. Availability of PEVs will be identified by their arrival time to home/work parking and departure time from home/work for home/work V2G scenarios. Assuming N PEVs with full-charged battery at home departure moment, the arrival state of charge ($SOC^i_{arrival}$) of the i^{th} PEV battery can be estimated as follows:

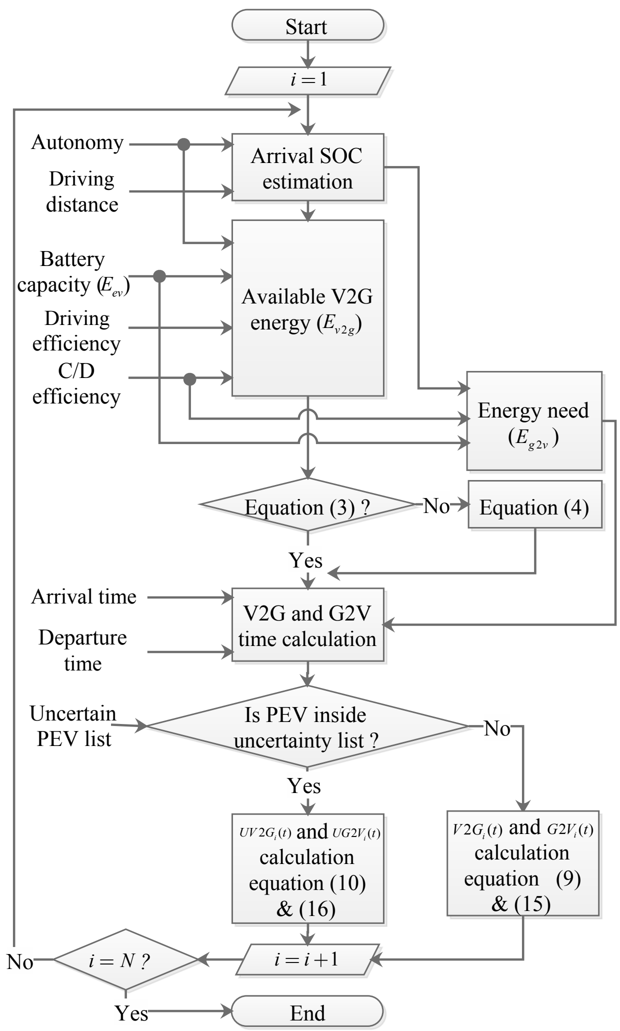

Fig. 4: The flowchart of AVPM.

$$SOC^i_{arrival} = (1 - \frac{D^i_d}{A^i}) \times 100\% \quad (1)$$

This is under the assumption of linear SOC drop with travel distance [41]. D^i_d denotes the driving distance of i^{th} PEV from home to work for work scenario and round trip for home scenario. The probability densities of arrival time ($T_{arrival}$), departure time ($T_{departure}$) and driving distance (D_d) have been presented in the previous section. In this section, the steps to model AVP are presented. The interdependency of these stochastic variables and their impacts on AVP will be analyzed afterwards. In current calculation, the averaged correlation coefficients are considered, where their calculations will be explained in MMSV block section. After the SOC estimation, Available V2G energy should be estimated for each V2G scenario.

$$E^i_{v2g} = (DoD \times E_{ev} - \frac{D^i_d}{\eta_{ev}})\eta_{cd} \quad (2)$$

For estimated V2G energy the following constraint should be satisfied:

$$2E^i_{v2g} + \frac{D^d_i}{\eta_{ev}} \leq T^i_{plug-in} \times P_{ch} \quad (3)$$

Where $T_{plug-in}$, is the plug-in interval of the PEV. If constraint (3) is not satisfied, the V2G energy should be recalculated as follows:

$$E^i_{v2g} = \frac{(T^i_{plug-in} \times P_{ch})}{2} - E^i_{g2v} \quad (4)$$

For office scenario, we consider the vehicle needs to have the same amount of energy as it has already consumed for arrival at work, plus 20% SOC to limit DOD at 80%.

$$E^i_{v2g-work} = (DoD \times E_{ev} - \frac{2D^i_{d-work}}{\eta_{ev}})\eta_{cd} \quad (5)$$

The duration of V2G and G2V action can be easily calculated by dividing the energy by charging/discharging rate:

$$T^i_{v2g} = \frac{E^i_{v2g}}{P_{ch}} \quad (6)$$

$$T^i_{g2v} = \frac{E^i_{g2v}}{P_{ch}} \quad (7)$$

After identifying the V2G and G2V energy, the planning should be applied. The charging and discharging planning should be done in a way to have maximum difference and minimum overlap between V2G and G2V power curves. The reason behind this choice is to be able to estimate the maximum achievable V2G power capacity of the fleet. This leads to analyze the potential services with respect to the maximum achievable V2G power of each bidding capacity, which will be presented afterwards. Overlapping of V2G and G2V power or mixed planning, i.e. charging/discharging at the same time horizon, leads to reduced V2G capacity of the fleet from aggregator capacity point of view. For home V2G planning, the plug-in interval ($PI_i(t)$) and V2G interval ($V2G_i(t)$) are defined as follows:

$$PI_i(t) = \begin{cases} 1, & T^i_{arrival} < t < T^i_{departure} \\ 0, & elsewhere \end{cases} \tag{8}$$

$$V2G_i(t) = \begin{cases} 1, & T^i_{arrival} < t < T^i_{arrival} + T^i_{v2g} \\ 0, & elsewhere \end{cases} \tag{9}$$

It means that, the PEVs are asked to be discharged upon their arrival, to have time to be fully charged up to departure time. In fact, after discharging period the PEV has time to recharge its battery and being full-charged for departure.

We define here the uncertain V2G time vector to complete formulation, where the complete approach to the uncertainty modeling is explained in the next section. Uncertain V2G time vector is:

$$UV2G_i(t) = UA_i(t) \times PI_i(t) \times V2G_i(t) \tag{10}$$

Where $UA_i(t)$, is the unavailability vector and the output of PAUM block. We define γ as the uncertainty coefficient, the portion of PEVs fleet, which have uncertain behavior potential.

$$K = \gamma \times N, \forall K \in Q \tag{11}$$

$$M = N - K, \forall M \in E \tag{12}$$

Where Q is the integer set of uncertain PEVs numbers, and E is the integer set of certain PEVs, where the following law is consistent:

$$E \cup Q = N \tag{13}$$

Finally, the V2G power called AVP for home scenario is as follows:

$$P_{v2g}(t) = \sum_{i=1}^{K} (UV2G_i(t) \times P_{ch}) + \sum_{i=1}^{M} (V2G_i(t) \times P_{ch}) \tag{14}$$

The G2V interval for calculation of G2V power should be defined as follows:

$$G2V_i(t) = \begin{cases} 1, & T^i_{departure} - (T^i_{g2v} + T^i_{v2g}) < t < T^i_{departure} \\ 0, & elsewhere \end{cases} \tag{15}$$

Uncertain G2V time vector is necessary for uncertain PEV and is obtained using:

$$UG2V_i(t) = UA_i(t) \times PI_i(t) \times G2V_i(t) \tag{16}$$

Using uncertain G2V vector and G2V vector, the G2V power of the fleet is estimated by using equation (17):

$$P_{g2v}(t) = \sum_{i=1}^{K}(UG2V_i(t) \times P_{ch}) + \sum_{i=1}^{M}(G2V_i(t) \times P_{ch}) \tag{17}$$

The final output of this block for a case of 1000 PEV fleet is depicted in Fig. 5 and 6. The potential bidding capacities from AVP at home and office are explained afterwards.

5.2. Bidding capacities (BC)

Based on the distribution function of arrival time, we have proposed three indicative intervals, so-called "potential interval (pi)", where there is a considerable cumulated number of PEVs and the V2G capacity of the fleet can be contracted. These three capacities, proportional with the number of available PEVs, are called bidding capacity for service market participation. We define the bidding capacity z, $(1 \leq z \leq 3 \in \mathbb{N})$ and its function, $BC_z(t)$, with its capacity value, Cap_z during its interval from t_1 to t_2.

$$BC_z(t) = \begin{cases} Cap_z, & t_1 < t < t_2 \\ 0, & elsewhere \end{cases} \tag{18}$$

The three indicative times have been chosen in order to propose biding start times BS_z for each bid as follows:

$$BS_z = \begin{cases} \mu - \sigma, & z = 1 \\ \mu, & z = 2 \\ \mu + \sigma, & z = 3 \end{cases} \tag{19}$$

The potential interval for each bid will be started from bidding start time until the power capacity equals to $BC_z(BS_z)$ as it is shown in the figures for both scenarios. In the Fig. 5, the V2G power called AVP, is starting right after the availability of the fleet shown in form of the arrival time histogram. It increases up to its maximum value corresponding to the whole fleet available PEVs, which is 3.7 MW active power. Due to the constraints of the PEVs such as, maximum battery DoD and their availability interval, the AVP decreases to zero until around 22:00 PM. The G2V power which corresponds to PEVs charging is completely separated from V2G power starting from 2:00 AM ending by the departure of the whole fleet at around 9:00 AM. From the modeled AVP, three candidates bidding capacities are extracted with the characteristics represented in Table. 4. In Fig. 6, the AVP is modeled with the same strategy while the constraints are minimum required energy for return trip and minimum battery DoD. These two modeled AVPs will be analyzed for V2G A/S potential assessment.

6. Multivariate Modeling of stochastic variables (MMSV)

In the probabilistic analysis with stochastic variables, the correlation between the variables should be taken into account even by knowing the marginal distribution of each single variable to avoid inconsistent

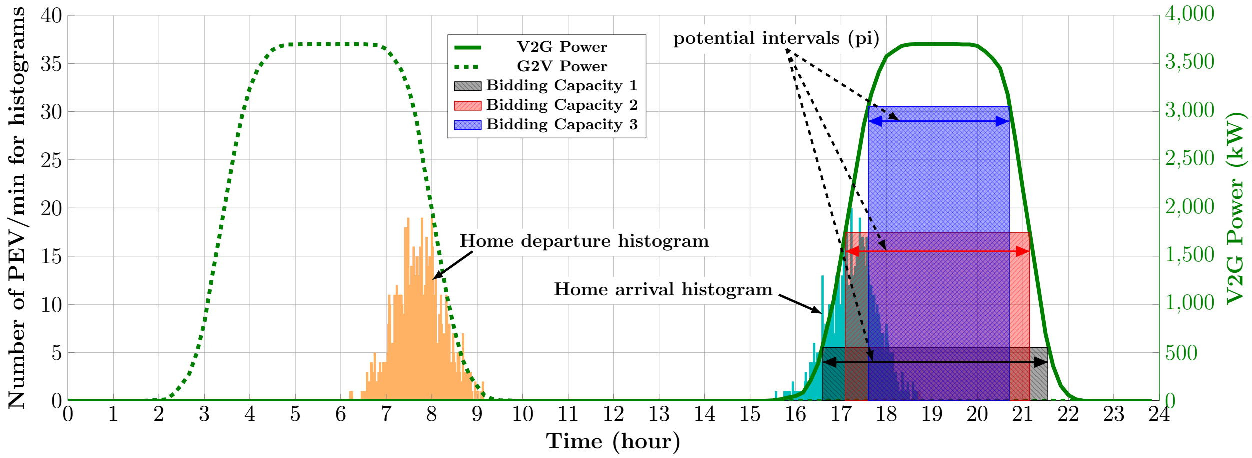

Fig. 5: The output of AVPM algorithm for home scenario, a fleet of 1000 PEV.

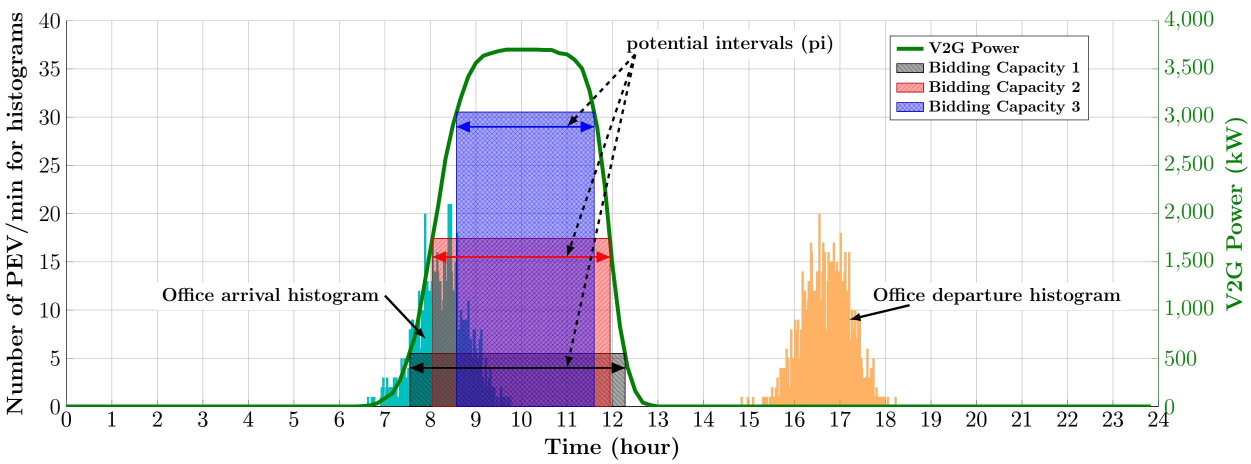

Fig. 6: The output of AVPM algorithm for office scenario, a fleet of 1000 PEV.

and unreliable estimation [42]. For the PEV fleet of daily home-work commuting, dependency of their departure times, arrival times and driving distances should be taken into consideration as they have key roles in modeling AVP and V2G energy capacity. However, the correlation between these stochastic variables can be estimated through statistical data as in [43] but their dependency impact on AVP and V2G energy should also be considered to provide a reliable marginal power capacity for aggregators. The latter is the case of this section. These dependencies can be analyzed with copula function. The approach of generating correlated samples using t copula sampling process is used in this paper where the notion and copula-based sample generation are explained thoroughly in [43]. t copula is used as it has tailed dependence modeling ability and is more suitable for real data modeling [43].

6.1. *The t copula*

A d-dimensional copula C is a d-dimensional distribution function on $[0,1]^d$ with standard uniform marginal distributions [44]. For each random variable x, copula functions are used to correlate univariate

Table 4: Bidding capacities' characteristics for home and office scenarios.

Scenario	BC1		BC2		BC3	
	pi (h)	Power (kW)	pi (h)	Power (kW)	pi (h)	Power (kW)
Home Scenario	5.5	550	4.2	1750	3	3050
Office Scenario	5.2	550	4	1750	2.9	3050

marginal cumulative distribution functions (CDF), $F_1(x_1)$, $F_2(x_2)$, ..., $F_d(x_d)$, to their joint CDF, $F(x_1, x_2, , x_d)$ [43]:

$$C(F_1(x_1), F_2(x_2), ..., F_d(x_d)) = F(x_1, x_2, ..., x_d) \tag{20}$$

Conversely, any copula C can be used to join any type of marginal distribution and construct a multivariate distribution function with the same marginal. The unique t copula for any uniform random variable $u = (u_1, u_2, ..., u_d) \in [0,1]^d$ is given by:

$$C^t_{\nu,P}(u) = \int_{-\infty}^{t_\nu^{-1}(u_1)} \int_{-\infty}^{t_\nu^{-1}(u_2)} \cdots \int_{-\infty}^{t_\nu^{-1}(u_d)} \frac{\Gamma(\frac{\nu+d}{2})}{\Gamma(\frac{\nu}{2})\sqrt{(\pi\nu)^d\,|P|}}(1+\frac{x'P^{-1}x}{\nu})^{-\frac{\nu+d}{2}}dx \tag{21}$$

Where t_ν^{-1} denotes the inverse CDF function of a standard univariate t_ν distribution with degree of freedom ν and symmetric positive definite correlation matrix P with unity diagonal elements.

6.2. AVP variation calculation

Generally, using the historical data or datasets gathered from statistical surveys, the correlation between arrival/departure time and driving distance can be easily estimated by fitting the multivariate distribution function to the datasets. This approach leads to the extraction of correlation matrix elements, which are representative of correlation degree between each two single marginal distribution [43]. In this study, an approach is proposed to quantify the impact of stochastic variable's dependencies on AVP. Afterwards, the correlation matrix elements associated with average AVP variation are considered as the case study. We assume that the working hours are fixed for whole fleet. In this case the dependency of the variables rationally should be either blue or red transition lines between possible linguistic correlations' states defined in Fig. 7. While, the other transitions will not provide reliable samples to take into account for daily home-work driving pattern estimation. It means that, for a PEV departing soon from home and arriving late to home, the driving distance should have been long and vice versa.

These correlations frame, present a linear direct correlation between driving distance and arrival time and a linear indirect correlation between departure and arrival time. Using a t copula function, the univariate marginal distribution of departure, arrival and driving distance can be related to their joint distribution as follows:

$$C(F_1(T_{departure}), F_2(T_{arrival}), F_d(D_d)) = F(T_{departure}, T_{arrival}, D_d) \tag{22}$$

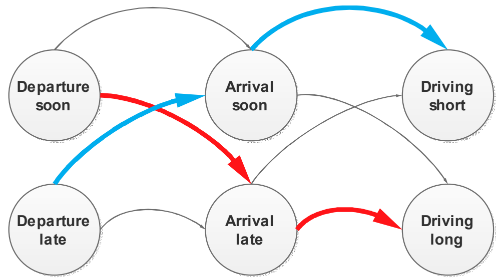

Fig. 7: Possible correlation states' transitions.

Considering the possible mentioned transitions, the elements of correlation matrix P will vary as follows:

$$P_{3\times3} = \begin{bmatrix} 1 & \rho_{12} & \rho_{13} \\ \rho_{21} & 1 & \rho_{23} \\ \rho_{31} & \rho_{32} & 1 \end{bmatrix} \tag{23}$$

where,

$$\begin{aligned} \rho_{12} = \rho_{21} &\in [-1, 0] \\ \rho_{13} = \rho_{31} &\in [-1, 0] \\ \rho_{23} = \rho_{32} &\in [0, 1] \end{aligned} \tag{24}$$

Where ρ_{12} indicates the correlation between departure time and arrival time, ρ_{23} indicates the correlation between arrival time and driving distance and ρ_{13} denotes the correlation between departure time and driving distance. In order to measure the sensitivity of AVP to the different possible correlation, an optimization approach is proposed where the variables will be the correlation matrix elements associated with maximum variation of AVP;

$$\min_{\substack{\rho_{12},\rho_{23},\rho_{32} \\ \rho'_{12},\rho'_{23},\rho'_{32}}} \left(\sum \left|P^{w}_{v2g}(t) - P^{v}_{v2g}(t)\right|\right)^{-1} \tag{25}$$

Subject to:

$$\begin{aligned} \{\rho_{12}, \rho_{13}, \rho'_{12}, \rho'_{13}\} &\in [-1, 0] \\ \{\rho_{23}, \rho'_{23}\} &\in [0, 1] \\ x^T P x &\geq 0 \end{aligned} \tag{26}$$

Where w and v are the two extreme cases of AVP affected by possible correlation between variables. The last constraint checks if the correlation matrix is positive definite or not for any possible x. This approach is tested on home V2G scenario as the case study where it is applicable on work V2G scenario as well. The results of optimization are brought in Table. 5.

Using the obtained results, the AVP of the two extreme cases is calculated where these two cases will never happen (Fig. 8). Considering the realistic case, there is always a correlation between three variables.

Table 5: Results of optimization for effect of correlation coefficients

Parameter	ρ_{12}	ρ_{13}	ρ_{23}	ρ'_{12}	ρ'_{13}	ρ'_{23}
Optimum value	-0.3960	-0.4950	0.99	-0.5940	-0.6930	0

The average value considered as the case study while in real case, the statistic's data or smart metering communication data can help to estimate the best correlation coefficients. The results show that the peak of AVP during its *pi* is the same for all three cases and there is only a negligible variation in power descending period.

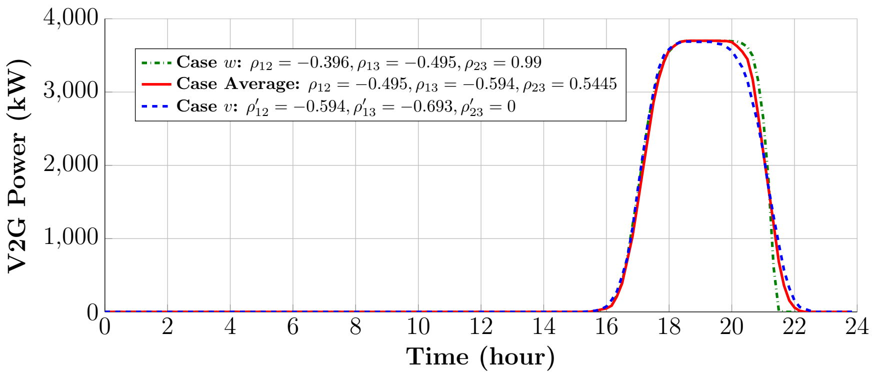

Fig. 8: Effect of various possible correlation between stochastic variables on the AVP.

In this paper, the parameters for average variation of AVP are considered as the case study, where the impacts of correlation between variables are illustrated in Fig. 9. As it is shown, the marginal distributions for both non-correlated and correlated variables are approximately the same, while the orientation patterns in 2D copula surface between each pair of stochastic variables are different. The orientation differences are justifiable considering the correlation states transitions shown in Fig. 7. In other word, the vehicles departing soon in the morning have potential to arrive late as they have had longer driving distance and *vice versa.* This effect is considered in AVP modeling procedure. The other effect, coming from unpredictable availability uncertainties, which is modeled using a probabilistic model, is explained in the next section.

7. Probabilistic availability uncertainty modeling (PAUM)

Availability uncertainty can have different reasons: Later arrival or sooner departure compared to the estimated or declared arrival and departure time, sudden departure in case of an urgent during the plug-in interval or any partial unavailability due to the leisure motives. Whatever the case, the PEV's unavailability from the aggregator point of view will be considered as V2G power unavailability and will impose negative impacts on contracted bidding capacity. Therefore, it is necessary to take into account the availability uncertainty factor prior to the capacity announcement.

The PEVs unavailability during their plug-in interval is highly stochastic and difficult to model. How-

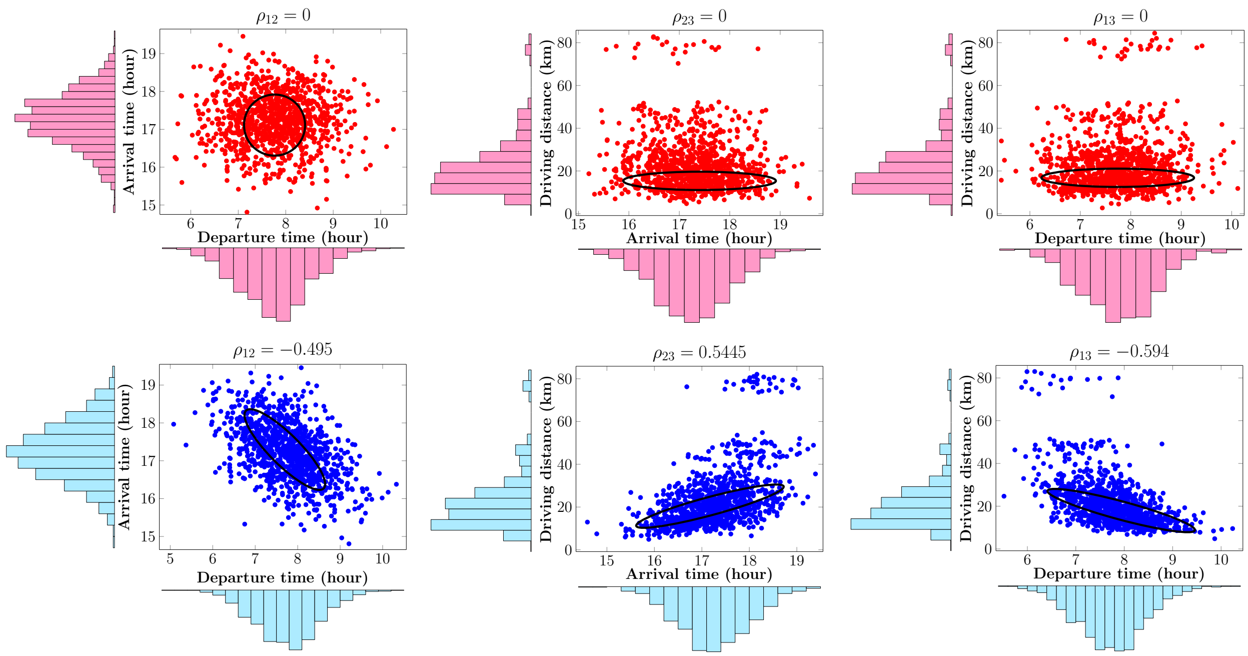

Fig. 9: Upper subplots: non-correlated stochastic variables, Lower subplots: correlated stochastic variables with averaged coefficients (Considered as the case study for AVP calculation).

ever, its stochastic nature follows a particular probability distribution which can be detected in daily trips percentage data. In this paper, an approach is proposed to model availability uncertainty knowing only the daily trips percentage and the fact that the trips leading to unavailability are included in trips probability distribution. Two parameters have been considered for each PEV in order to model its unavailability:

1. Departure moment as $T_{depstart}$
2. Unavailability period as DUR_{UN}

In addition, an uncertainty coefficient has been introduced as, $\gamma = [0, 1] \in \mathbb{R}$, which is the portion of PEVs fleet, that have potential of availability uncertainty. In another word, $\gamma = 1$, means that all of the PEVs inside the fleet will experience at least a short departure during the plug-in time. Monte-Carlo simulation (MCS) is used to generate samples with given trips percentage and prepare inputs for Gaussian mixture model (GMM) with a given number of components. Two major Gaussian components will be considered as trips related to departure from home to work in the morning and departure from work to home in the afternoon. By filtering these two components, the probability of the other motives' trips leading to availability uncertainty can be detected. In the second step, using a uniform distribution by lower bound as home arrival time and upper bound as V2G interval, the sampling process of $T_{depstart}$ will be bounded over V2G interval and conducted by filtered GMM probability distribution. For DUR_{UN}, sampling a uniform distribution between 30 minutes to 3 hours is used. This is the maximum time length a PEV will be unavailable based on the mobility survey information. In this approach, we assume that the amount of PEV battery energy used during the unavailability interval is the same as the energy amount that would be provided as V2G, if PEV was available in the parking. In the following, the formulation of different steps of the approach is provided along with the modeling framework in Fig. 10.

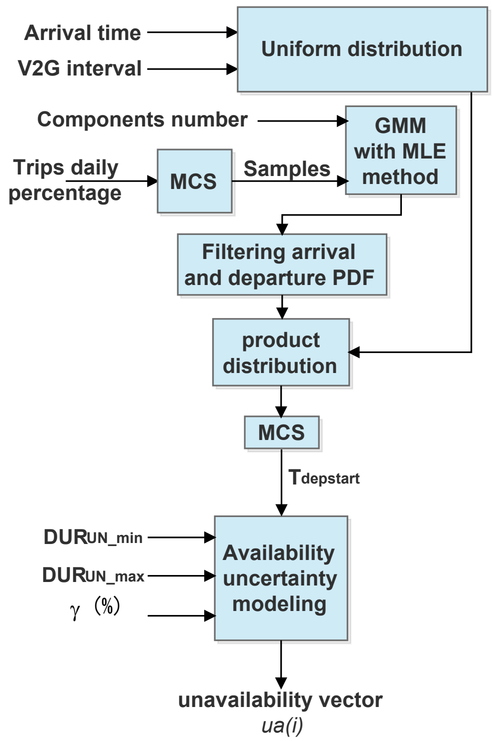

Fig. 10: The PAUM framework.

7.1. Gaussian mixture model

In this study Mixture model is used to find the sub-populations of daily trips percentage to associate an availability uncertainty probability distribution to the unknown sub-populations. These sub-populations are modeled as Gaussian components in GMM. For this reason, MCS is used to provide samples based on daily trips percentage and their probability distribution is estimated using kernel density estimation. The estimated probability density is used in MLE in order to estimates the parameters of GMM components with maximum likelihood percentage (Fig. 11).

One-dimensional GMM density function for a set of C components and their parameter sets as $\Theta = (\alpha_1, \alpha_2, ..., \alpha_c, \sigma_1, \sigma_2, ..., \sigma_c, \mu_1, \mu_2, ..., \mu_c)$ is represented as follows [45];

$$f(x_s|\Theta) = \sum_{j=1}^{c} \alpha_j \frac{1}{\sqrt{2\pi\sigma_j^2}} exp(-\frac{(x_s - \mu_j)^2}{2\sigma_j^2}) \tag{27}$$

We assume that $\alpha_j \geq 0$, for $j \in [1, ..., c]$ and $\sum_{j=1}^{C} \alpha_j = 1$. x_s represents the samples. The best likelihood is obtained with 6 components with parameters shown in Table. 6.

The last two components can be considered as trips related to departure from home to work in the morning and departure from work to home in the afternoon since their parameters are near to the ones which have

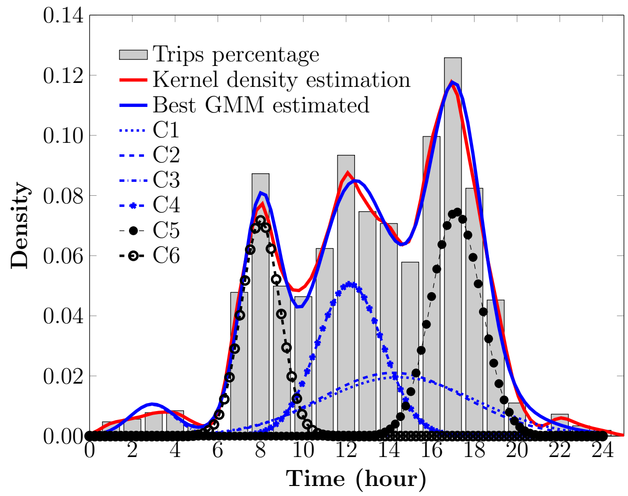

Fig. 11: Kernel density fitted to trips percentage along with best GMM fit with 6 components.

Table 6: parameters of GMM components.

Component j	C_1	C_2	C_3	C_4	C_5	C_6
$\mu_j(hh:mm)$	14:27	14:13	02:55	12:25	17:08	08:00
$\sigma_j(minutes)$	217	202	63	92	45	36

been considered in the previous section. By filtering these two components from GMM, the density function of other motives trips can be found (Fig. 12).

7.2. Uniform distribution

Using a uniform distribution, the sampling process for parameter $T_{depstart}$ can be bounded on the V2G time interval in order to emphasize uncertainty over AVP. In flexibility study in the next section, the interval will be adapted by a flexibility interval. The filled intervals in Fig. 12 show the products of uniform distribution and filtered GMM density function, which will be considered as uncertainty density function for uncertainty sampling process. In other words, the sampling process will be done randomly considering the obtained uncertainty density as the probability of selection. This density function can be represented as follows:

$$g_{un}(x_s|\Theta) = \begin{cases} \sum_{j=1}^{4} \alpha_j \frac{1}{\sqrt{2\pi\sigma_j^2}} exp(-\frac{(x_s-\mu_j)^2}{2\sigma_j^2}) & T_{arrival} < x_s < T_{arrival} + T_{v2g} \\ 0 & elsewhere \end{cases} \tag{28}$$

Where $T_{arrival}$ will be arrival time of first PEV at work for work V2G scenario and at home for home V2G scenario. For the unavailability period, a uniform distribution is considered with cumulative distribution function as follows:

$$F(DUR_{UN}; a(i), b(i)) = \frac{DUR_{UN}(i) - a(i) + 1}{b(i) - a(i) + 1} \tag{29}$$

Where $a(i) = 30min$, $b(i) = 3hours$ and $DUR_{UN}(i) \in [a(i), b(i)]$. The outputs of the model for two scenarios are depicted in Fig. 12. This density function will be used as inputs for uncertainty sampling process, and it will affect the V2G vector as in (10). The impact of modeled uncertainty on each bidding capacity during its pi is studied using a reliability factor (RF), which is the ratio of available V2G energy with uncertainty divided by V2G energy without uncertainty. The results depicted in Fig. 13, show intensive impacts on BC3, particularly for home scenario. The BC1 remains mostly reliable even with the highest γ value. This analysis helps to choose the most reliable BCs where the procedure will be completed by assessing the flexibility of each BC in next section.

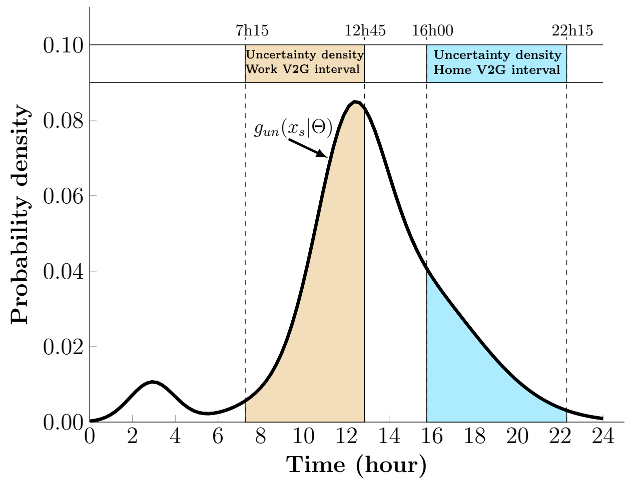

Fig. 12: Uncertainty probability density function for two V2G scenarios at work starting from 7h15 and at home starting at 16h00.

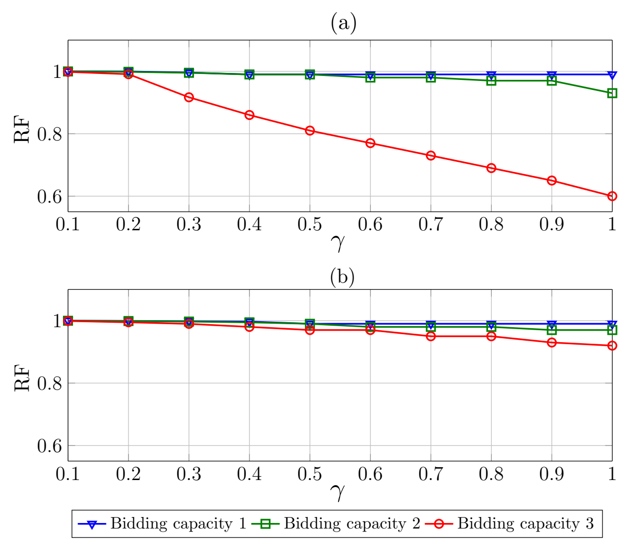

Fig. 13: Impact of uncertainty on reliability factor for, (a) home scenario, (b) work scenario.

8. Bidding flexibility calculation (BFC)

As we modeled the AVP upon the arrival of the PEVs, it would also be possible to coordinate the discharging time in order to prolong the bidding capacity interval. This so-called "bidding capacity flexibility" is analyzed in this section under a stochastic global optimization problem approach. Considering the BCs defined in previous sections by (18) and (19), the only way to maximize these capacities is to maximize the potential interval and for this goal, the only degree of freedom is to coordinate the V2G time of PEVs.

8.1. Flexibility problem formulation

The purpose of this optimization is to maximize the BC time interval, starting from its availability. For instance, for bidding 1 starting at 16h45, the objective is to maximize the capacity interval using V2G start time coordination of PEVs. This maximization is under constraints of respecting the G2V capacity of the fleet (for home scenario) and possible flexible range of V2G start time. In order to simplify the calculation one parameter per PEV is considered, and it is the V2G start time which varies between arrival time and G2V start time minus V2G time interval. We define the $k(t)$ function as the counter of sample times having a capacity more than each BC.

$$K(t) = \begin{cases} 1 & P_{v2g}(t) \geq BC_z(t) \\ 0 & elsewhere \end{cases} \tag{30}$$

Objective function:

$$\max_{T_{VS}(i,i+1,\ldots,N)} \sum_{t_1}^{t_2} K(t) \tag{31}$$

Subject to:

$$\begin{aligned} P_{v2g}(t) \geq BC_z(t), \forall t \in [t_1, t_2] \\ T_{arrival}(i) \leq T_{VS}(i) \leq T_{departure}(i) - T_{g2v}(i) - 2 \times T_{v2g}(i) \end{aligned} \tag{32}$$

Where $T_{VS}(i)$ is the V2G start time of PEVs arriving after BS_z that should be coordinated in order to maximize the available interval of $BC_z(t)$. Considering the normal distribution empirical rule (three sigma) and number of PEVs per fleet, the number of parameters that has to be optimized can be calculated as follows for a fleet with N PEV, $P_1 = 0.6827$ and $P_2 = 0.997$:

$$Param_{num} = \begin{cases} \frac{P_1+P_2}{2} \times N & z = 1 \\ 0.5 \times N & z = 2 \\ \frac{P_2-P_1}{2} \times N & z = 3 \end{cases} \tag{33}$$

For instance, for a fleet with 1000 PEV, in order to calculate flexibility of bidding $z = 1$, 838 parameters correspond to the PEVs arriving after BS_1 should be optimized. This expression shows that we face with a relatively large optimization problem which needs a powerful algorithm.

8.2. Methodology

The major challenge for this optimization problem is finding the best feasible solutions (global optimum), knowing the potential of high dimension problem and stochastic nature of the problem, which makes difficult to use deterministic and gradient based optimization algorithms. The latter using derivative free algorithms seem effective. In [46], it is shown that Free Pattern Search (FPS) algorithm is scalable to the dimension increasing and performs better compared to the other evolutionary algorithms. This algorithm employs the HJPS method as a local search algorithm and two operators from FS to guarantee the diversity of search in order to inherit the global search. Long et al. showed that FPS has very fast convergence speed, better solution accuracy, swarm management ability and robustness to the dimension compared to the similar evolutionary algorithms.

In this paper, we have implemented FPS algorithm on bidding flexibility problem, and its functionality is assessed in both quality of result and dimension increment.

8.3. Free Pattern search

FPS is a population-based global optimization algorithm with three main parts; initialization, exploration and termination. In exploration part, there are three operators: search operator for local search based on HJPS, acceleration operator to avoid trapping in local optimums and a throw operator, which ensures the diversity of population. A single individual, $X_j, \{1 \leq j \leq m \in \mathbb{N}\}$, will do the search based on HJPS algorithm in all of its dimensions, $1 \leq i \leq n \in \mathbb{N}$, bounded between lower and upper limits, Low_i and Up_i. The flowchart of the FPS algorithm is illustrated in Fig. 14 and the different operators are explained afterwards.

Search operator uses the HJPS algorithm to find local optimum for each individual. HJPS is a single-point search method which uses a pattern to search around the base point. There are three types of points in HJPS; the current point Ψ, the base point ϕ, and previous point θ. The current point is the actual solution of algorithm.The base point is for finding the better solution, and the previous point is the last current point. The HJPS contains two parts: exploration move (EMove) and pattern move (PMove). EMove will search in all dimensions of the base point to find the best trial. If the best trial is better than current point, the PMove will be implemented.

Acceleration operator separates the population in two groups. The first group are the individuals trapped in local optimum and need to be accelerated. Using a sensibility factor S, the individuals will be polarized into two groups and the first group individuals X_j^1 will be accelerated thanks to the randomly selected second group individuals X_r^2.

Throw operator detects the individuals that would gather and search in the same small space. It scatters them by adding or subtracting a $\Delta_{i,init}$ length to every dimension of the start position $X_{i_{start}}$ of gathered individuals. Throw operator keeps the population diversity in the search space. After finishing all operations the algorithm will be terminated facing with maximum step or maximum function call and accuracy of the solution.

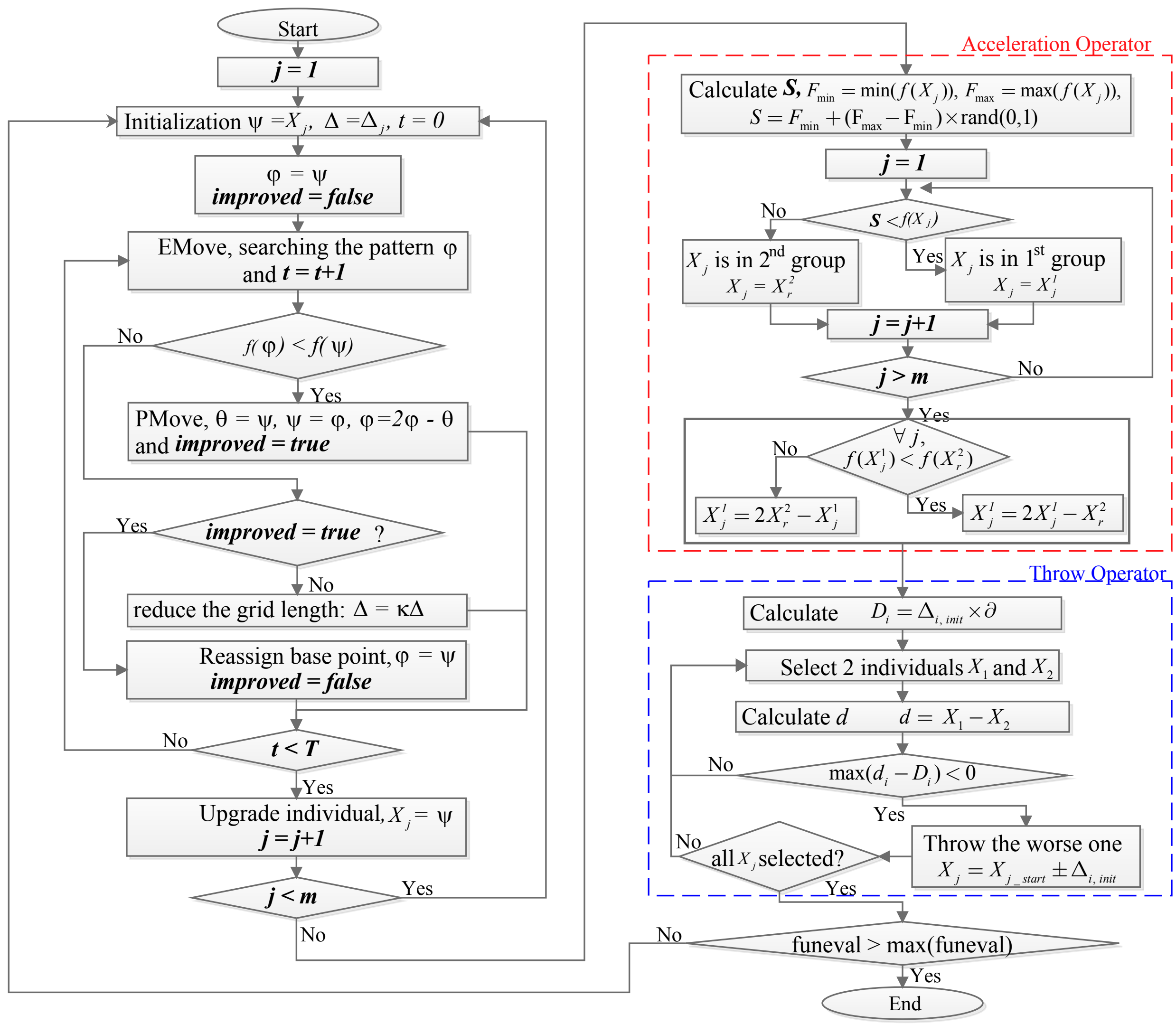

Fig. 14: FPS algorithm flowchart.

8.3.1. Results

The method is implemented on different PEV fleet numbers. Fig. 15 shows the function evaluation per all individuals for the fleet of 50, 200 and 500 PEVs. The result shows a complete convergence of all individuals for all cases. This shows the robustness of the algorithm to the dimension increment. The convergence and exploration intervals are indicated on the function evaluation windows. By increasing the dimension, the exploration is also prolonged. The optimization is stopped when all the individuals in each evaluation are converged to a single value and there is no further improvement in term of optimum result. The best value is obtained 10.5 hours. In fact, as the problem is stochastic, the optimization is repeated to have all cases with the same optimum values while the final results for bidding capacity 1 is almost around 10 hours for all the PEV fleet cases. This optimization is done in presence of different values of uncertainty coefficient, and the results are presented in Fig. 16. The impact of uncertainty shows a linearly drop on the flexibility interval and more important on home scenario biddings. The BC3 for both scenarios has a flexibility less than 3 hours after 20% uncertainty ($\gamma = 0.2$). It shows that BC3 compared to BC1 and BC2 has less reliability in terms of interval flexibility even by having a power more than them. Since the minimum time requirement for ancillary services discussed in this paper is 3 hours, the BC3 will not be considered in further analysis. Fig. 17 shows the flexibility of BC1 and BC2 with the uncertainty coefficient of $\gamma = 0$. In BC1, the flexibility algorithm reaches to prolong the potential interval of BC1 from 5 hours up to 10.5 hours. In BC2, the flexibility reaches 8 hours.

The flexible interval (fi) of each BC will be used for service assessment in the next section. The availability uncertainty is considered with $\gamma = 0.1$ in the further analysis. This value is estimated for the PEV fleet in Niort.

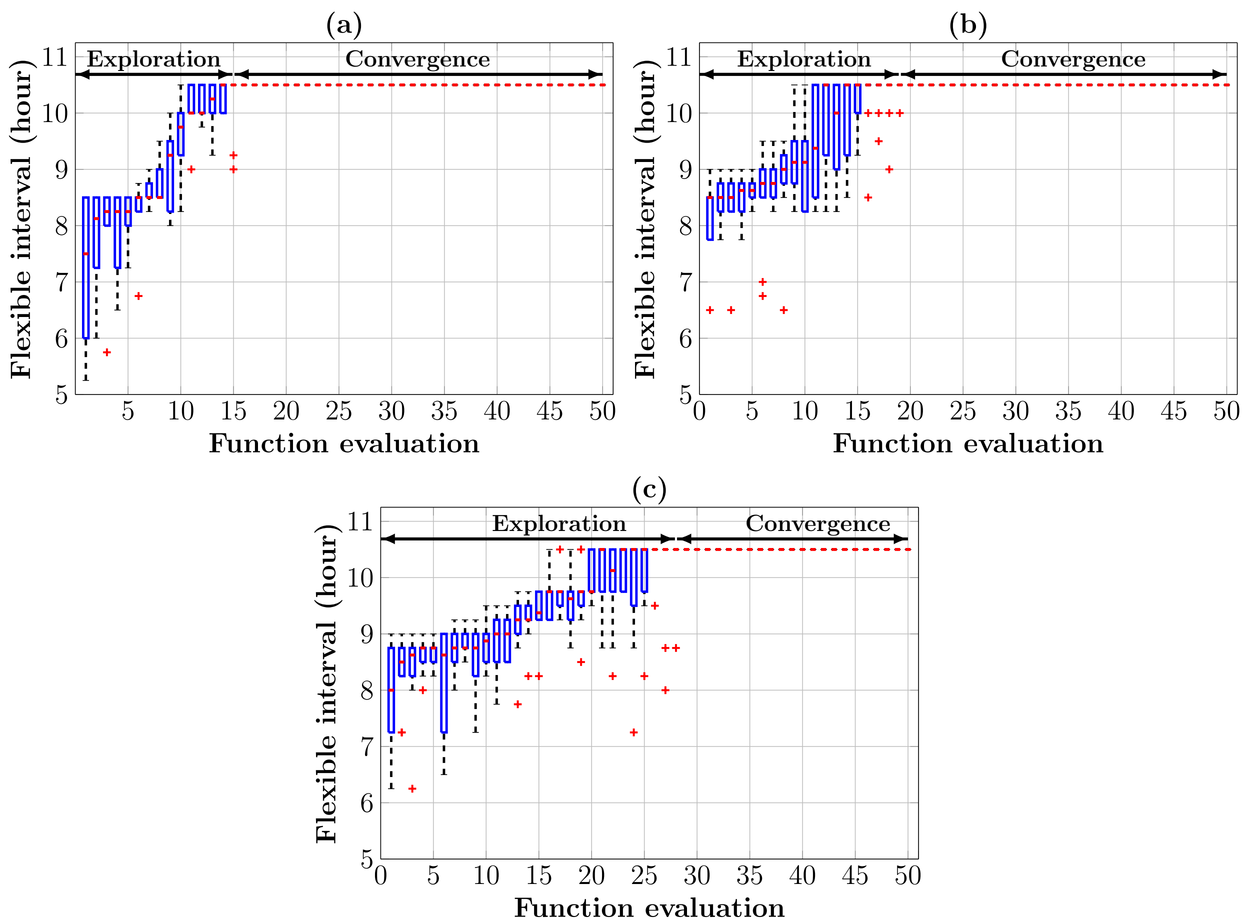

Fig. 15: Function evaluation (Individuals' boxplot per evaluation) for, (a) 50 PEVs fleet, (b) 200 PEVs fleet and (c) 500 PEVs fleet.

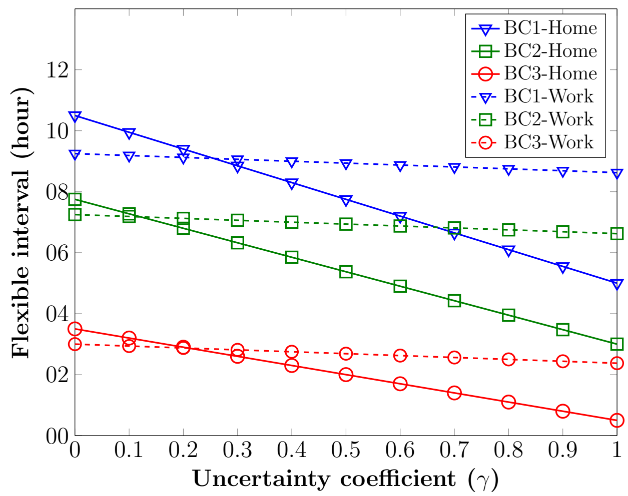

Fig. 16: Bidding flexibility vs. uncertainty for both scenarios.

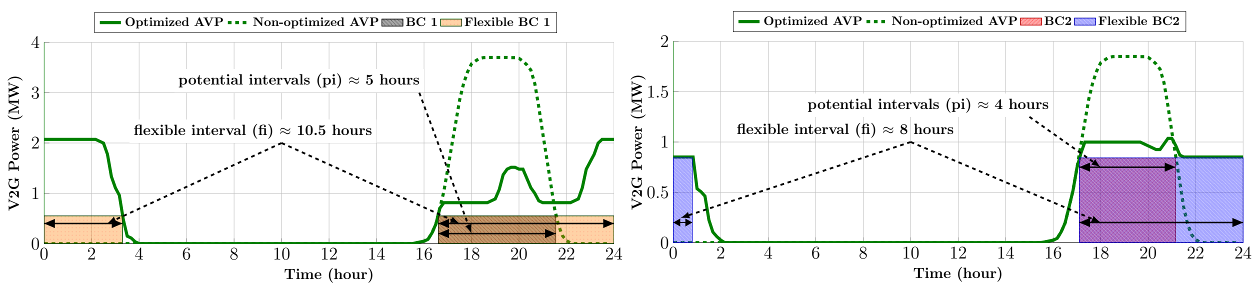

Fig. 17: Left plot: BC1 flexible interval, Right plot: BC2 flexible interval.

9. Ancillary service assessment

9.1. Ancillary services

In [27], a possible list of ancillary services for storage systems at the distribution grid level under the confirmation of main French DSOs is proposed. These services' feasibilities are analyzed also for PEVs in previous work of the authors [47]. In this paper, these services are evaluated for PEVs under an aggregation contract considering each service constraints. The active power based services presented in Table. 7 are chosen for this study. The first constraint for each service is the minimum amount of power, and minimum required time interval. These limits are used in order to design the fuzzy inference system for each service. Thanks to a service/localization matrix available in [27], the localization limitation of each service is also taken into account as another constraint. The utilization frequencies of the services, which depends on the nature of the service and the activation signals, are considered as the last constraint. In this study, three activation signals in form of a probability function are considered (Fig. 18). Annual averaged daily load profile (DLP) is considered as probability function for services sensitive to DLP variations. Annual averaged daily frequency *regulation up* signal is used for regulation services and finally, annual averaged daily balancing mechanism (BM) demand is chosen for BM service assessment. In the Table 8, the analyzed services in this study are introduced.

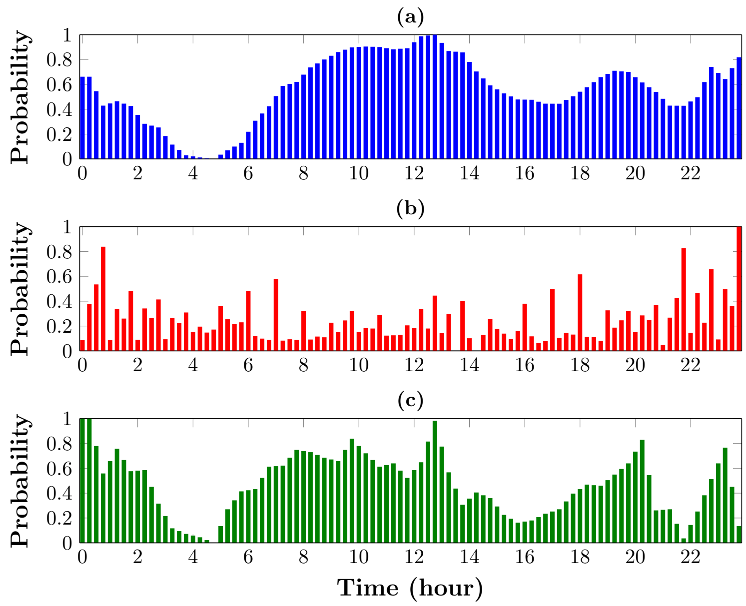

Fig. 18: Probability of activation signals for, (a) Daily load profile (DLP), (b) Frequency regulation up (RU), (c) Balancing mechanism up (BM).

Table 7: Ancillary services requirements for distribution grid [27, 48].

Service	Loc. limit	Min. Power (kW)	Max. Power (kW)	Min. time(h)	Activation signal
PPSMV	A	500	2000	3	DLP
PPSLV	C	100	500	3	DLP
VRMV	B,D	500	2000	3	DLP
VRLV	C	50	500	3	DLP
LM	A	100	2000	3	DLP
ETCM	A	2000	5000	3	DLP
FR	A	1000	5000	3	RU
BM	A	10000	15000	3	BM

9.2. Distribution grid service/localization limitation

At the distribution grid level, the effective potential place for each type of ancillary service is different. Reference [27], under the consultation of major French DSOs, proposes the different candidate locations for installing energy storage systems. These places are considered as the limit for the aggregated number of PEVs in order to assess the service potential. In this study, based on the chosen services, 4 candidate points are considered as the limits for each type of service (Fig. 19). **Point A** is at the topmost level of distribution grid in border of distribution and transmission grid. This point is considered as a HV/MV substation for

Table 8: Ancillary services characteristics for distribution grid.

Service	Characteristics
PPS	Peak Power Shaving is evaluated at both MV and LV grid. PEVs are charged during off-peak hours and discharged via V2G at peak hours. It provides economic interests for PEV owners, aggregators and DSO.
VR	Maintaining voltage in acceptable contractual/regulatory boundaries [49]. At MV feeder a few % of regulations needs at least 500 kW to 2 MW [48]. It is based on typical value of MV feeder impedance in French distribution grid. This study is only focused on the active power contribution on voltage regulation.
LM	Peak load should be avoided to minimize the losses. The line length, active and reactive power of the connected consumers are important for dimensioning the storage units.
ETCM	The DSO has to pay to TSO an annual bill related to energy transmission. Minimizing the bill with local produced renewable energy consumption and PEV charging coordination can be possible [38].
FR	Primary frequency regulation for French grid is 600 MW. A Minimum of 1 MW at the distribution grid level is required [50].
BM	Balancing Mechanism is a part of tertiary frequency control. The French producers and consumers having 10 MW available Power can participate in BM market [50]

the range of 63 to 225 kV for HV side and 15 to 20 kV for MV side. **Point B** is considered as the MV feeder level for feeders with 15 or 20 kV voltage level. **Point C** is considered as the LV bus bar inside the MV/LV substation for the range of 400 V in LV side. Finally, for industrial/professional customers possessing a private MV/LV substation, **Point D** is considered, which will be the case for office charging scenarios.

In fact, for each service, based on its localization limitation mentioned in the Table. 7 the aggregated number of PEVs fleet will be evaluated at that limit.

For our case study in Niort, a statistical analysis is done in order to discover the distribution of residential customers inside the distribution grid and for the 4 candidate locations. In point A, the possible number of PEVs for home scenarios are brought in Table. 9. For office scenario, 2841 PEVs can be aggregated up to the point A. The possible number of PEVs in Niort for each provision scenario are distributed between all MV/LV substations based on the residential consumers' distribution, inside the MV/LV substation (Fig. 20.a). Distributions of PEVs at the level of MV feeder for home scenario are brought in Fig. 20.b. The residential consumers are considered as the charging locations at home and for office scenario, the professional consumers are taken into account. For both scenarios, the maximum number of PEVs at each level of the grid are calculated considering the actual subscribed power for each consumer. It means that the capacities of the grid for hosting the PEVs are taken into consideration as constraints. For both evolution scenarios at home scenario, there is no case exceeding the subscription limitation. For office scenario, the maximum possible number of PEV before limitation violation are considered for study, as there is no evidence to justify

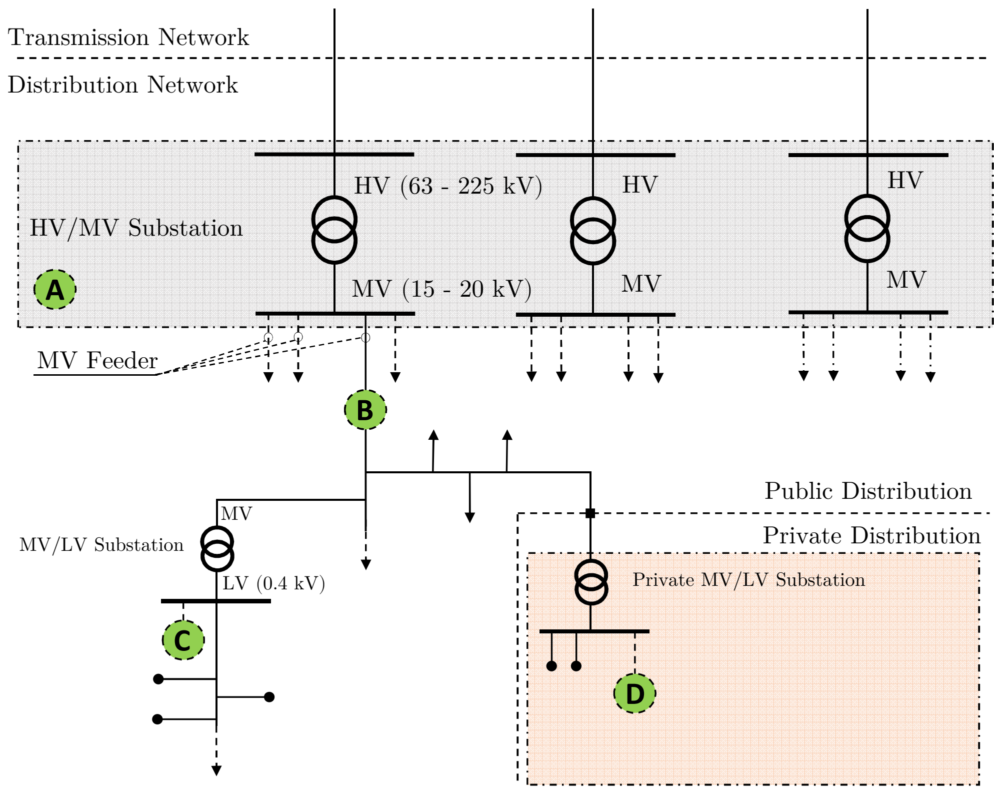

Fig. 19: Distribution grid schematic with location limitation for ancillary services.

the exact number of PEVs for office scenarios. It is due to the combination of traffic flow between Niort and its neighbor cities during the day. Their distribution at point B, C and D are brought in Fig. 20.c along with mean values considered in potential calculation.

Table 9: Aggregated number of PEVs up to HV/MV substation (point A) for home scenario.

Evolution horizon	2020	2025	2030
Low Scenario	681	1446	2127
High Scenario	1702	4680	7657

9.3. Fuzzy inference system service assessment

In order to assess the potential of PEV fleets for V2G ancillary services, a methodology is proposed. This method considers the bidding capacities characteristics of each fleet and compares it with potential probability of each service. A fuzzy inference reasoning system is designed to quantify the potential of each fleet and each bidding capacity for each particular ancillary service. As the services' requirements are defined by power and time in form of an interval, the assessment procedure seems to be in a fuzzy form as the exact evaluation also needs accurate requirement. For each service, minimum and maximum power need and time are identified in Table. 7. Two inputs are considered for this system. The first one is dedicated to time

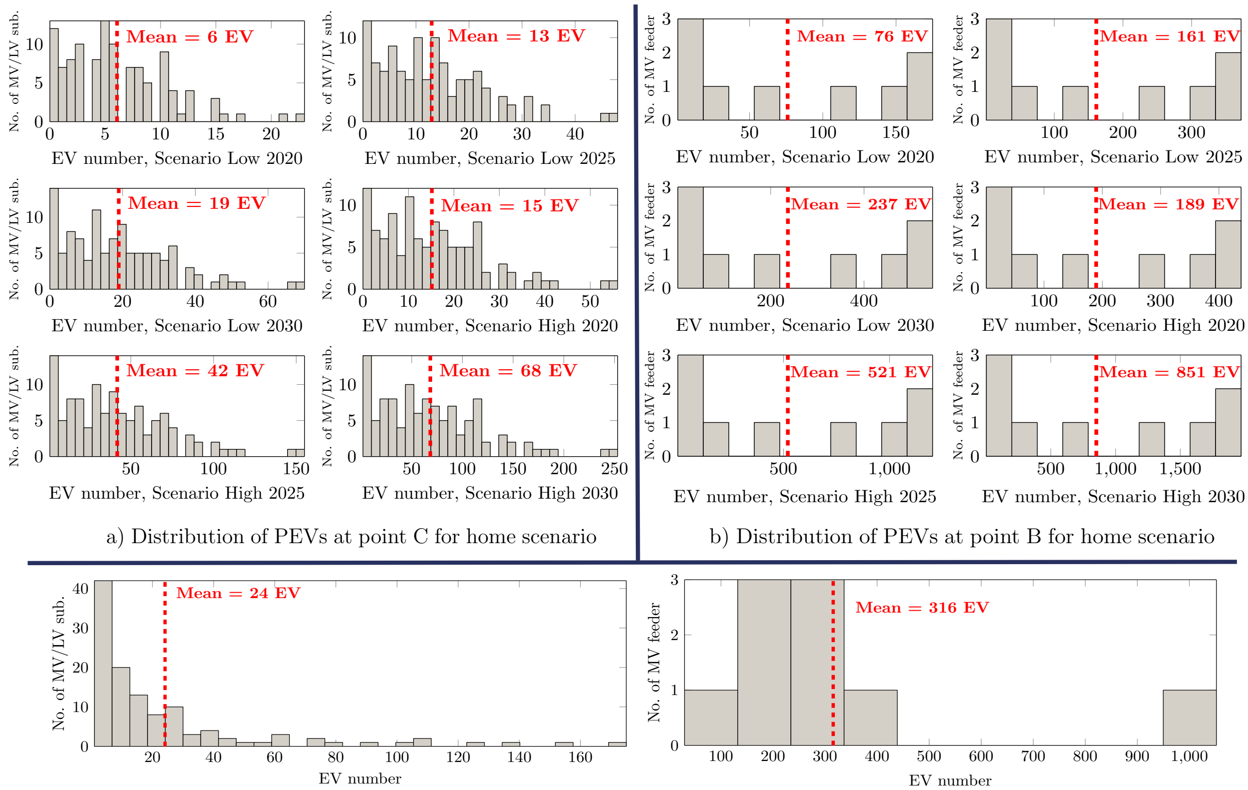

a) Distribution of PEVs at point C for home scenario

b) Distribution of PEVs at point B for home scenario

c) Distribution of PEVs at point B (MV feeder) and C/D (MV/LV substation) for office scenario.

Fig. 20: Distribution of PEVs at different points for home/office scenarios.

interval of each service that can be provided by that particular bidding capacity of the fleet. By considering the probability of the service as $ST(t)$ and probability of bidding capacity as $FT(t)$ the first input is defined as:

$$DUR = \sum_{t=1}^{24} FT(t) \times ST(t) \tag{34}$$

Probability of bidding is a vector with value 1 during the flexible interval (fi) of each bidding and 0 for other intervals of the day.

$$FT(t) = \begin{cases} 1, & BS_z \leq t \leq BS_z + fi_z \\ 0, & elswhere \end{cases} \tag{35}$$

This input is normalized using g factor as, $g = 1/\sum_{t=1}^{24} ST(t)$. The second input is the power that should be provided for each service. The membership function of this input will be made based on minimum and maximum required power for each service provided in the Table. 7. The example of inputs and output for service PPSMV is brought in Fig. 21.

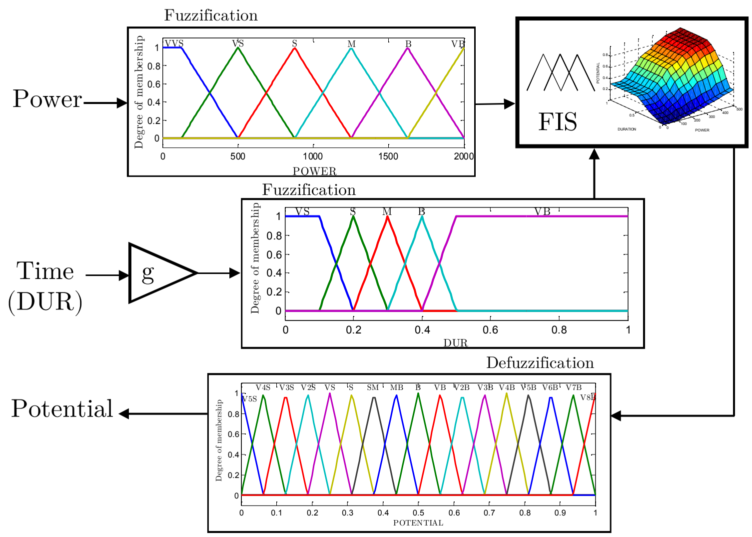

Fig. 21: FISSA algorithm, inputs and output example for service PPSMV.

10. Results and discussion

A graphical indicator is designed for potential comparison of different services and bidding capacities represented in Fig. 22 for home and Fig. 23 for office scenarios. For each BC a minimum potential factor called *BC limit* is calculated using minimum power of the services and flexible interval of the BC. This factor is considered as minimum requirement for each BC of the services and is represented in form of a dotted-dashed line with filled upward area. Based on this indicator, every fleet evolution scenario should be inside the BC filled area in order to be competitive for that service. Afterwards, the potential of the different fleets' evolution scenarios is assessed using their provided power associated with their aggregated number of PEVs at each service's candidate point.

For home scenario, the services PPSLV and BM are not competitive up to 2030 horizon unless for high scenario of BC2. However, the services PPSMV, LM and FR are mostly well adapted with the provisions. In FR service, the low scenario BC1 can be possible from 2030. For PPSMV, the low scenario BC1 is also possible from 2025. In ETCM service, low scenario BC1 is not at all competitive up to 2030. This is the same case for low scenarios BC1 and BC2 in VRLV and VRMV services.

For office scenario in Fig. 23, the services PPSLV, VRMV and BM are impossible. The services FR, LM and PPSMV are inside the area, so they can be competitive for the office fleet. The actual study shows that for BC1 the services VRLV and ETCM cannot be competitive. It should be taken into account that in this study, the numbers of PEVs at work are estimated based on actual grid capacity, and the studied volume availability is not at all guaranteed.

The results for both scenarios show that the services in the low voltage grid have not enough potential due to the non-sufficient number of aggregated PEVs at LV grid, i.e. mostly less than 30 PEVs in all provision scenarios. In addition, for service BM, due to its huge power capacity requirement, the fleets' provisions are

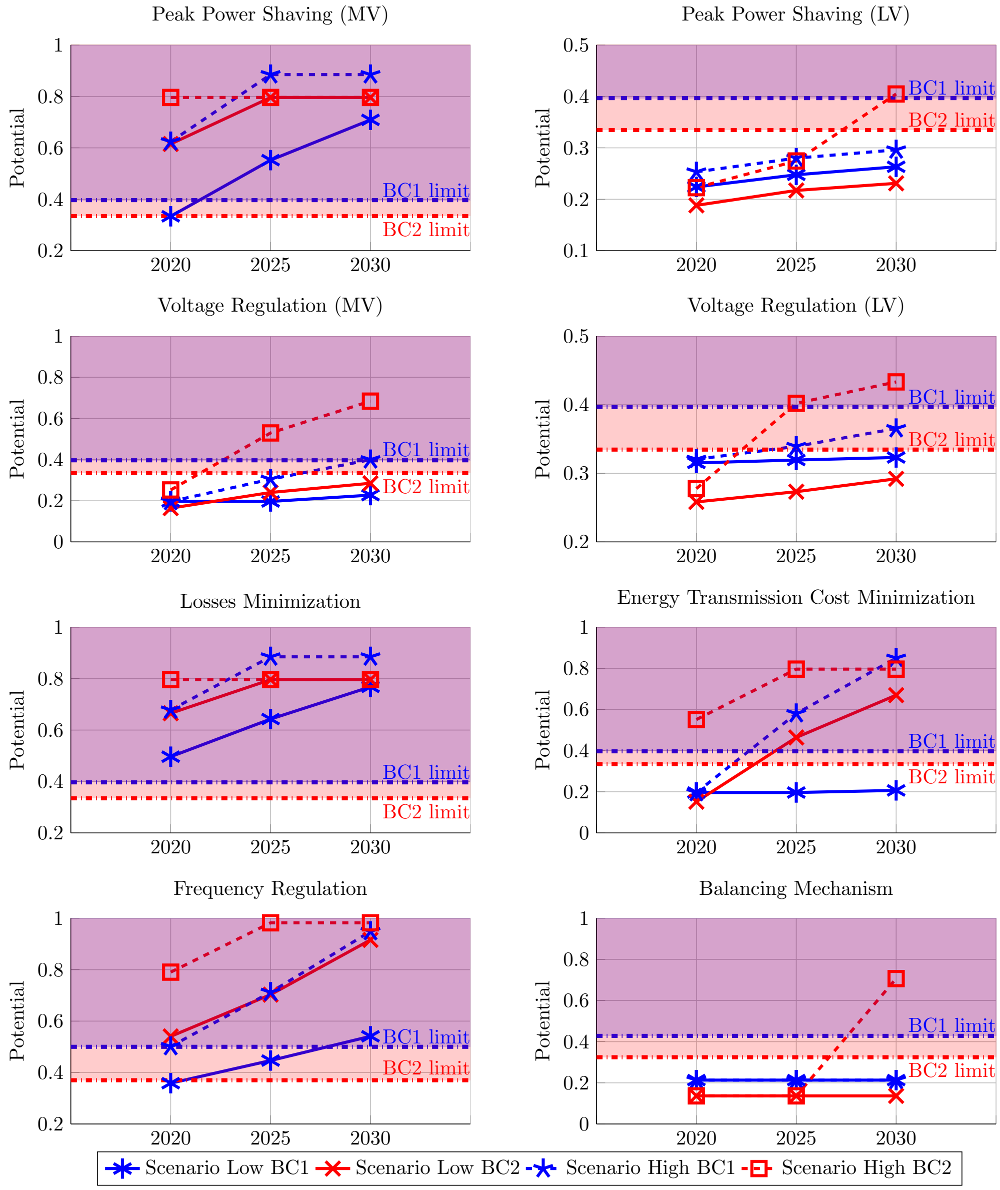

Fig. 22: Potential evaluation for home scenario under all evolution scenarios.

mostly not competitive as the available aggregated number of PEVs at point A cannot cover the BM service power capacity requirement.

The proposed approach provides the potential evaluation of V2G ancillary services for distribution grids. This approach is useful in V2G energy management modeling by concentrating on the main requirements and limitations of each particular case study. By utilizing the proposed approach, the V2G management system will be efficient and scalable to that specific case study. Furthermore, the real potential services can be listed based on their priorities, which would be practical in the energy management scheming's step. By knowing the flexible capacity of each V2G fleet, in the context of renewable energies' intermittent mitigation, the management systems can be efficiently dimensioned to the real capacity of the V2G fleet as well. The

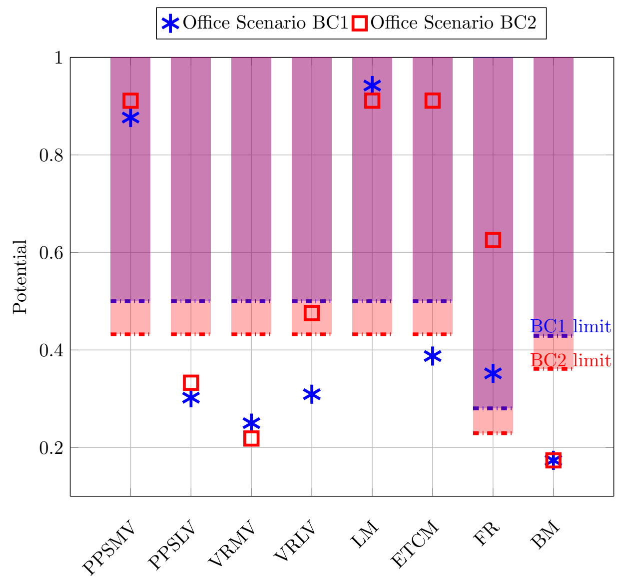

Fig. 23: Potential evaluation for office scenario with PEV number estimated upto the grid capacity (subscribed power limit).

proposed approach facilitates the choice of the proper ancillary services for V2G energy management and also increases the benefits from the services' mutualization for the aggregators.

11. Conclusion

V2G ancillary services potential assessment was discussed in this paper. The available V2G power of the PEV fleets doing daily home-work commuting was modeled. This modeling is based on stochastic data such as arrival/departure time and driving distance and averaged data, containing vehicle's characteristics. The interdependency of stochastic variables was analyzed using copula function. Two rarely discussed important factors affecting the AVP were also modeled and their impacts on AVP were identified. Availability uncertainty of the PEVs during their plug-in interval was modeled using only daily trips percentage and its decomposition thanks to the Gaussian mixture model. Secondly, the service localization limitation was considered in the procedure of V2G service assessment of the PEVs fleet.

The impacts of availability uncertainty were studied on three potential bidding capacities for both home and work scenario. The results indicated that the biddings in work places are more reliable than biddings at home as the probability of uncertainty has less concentration during the work plug-in time compared to the one at home. The flexibility of each bidding capacity was calculated using a robust global optimization technic. The impacts of uncertainty also showed linearly drops on flexibility intervals and generally fewer negative impacts on work biddings' flexibility intervals compared to home scenario. Using the obtained flexible interval for each bidding capacity and V2G power of each PEV fleet, the potential of ancillary service participation of the fleets was studied thanks to a fuzzy inference system. The fuzzy system lets to quantify the potential of each fleet considering the requirement of the services such as minimum power and time and localization limitation of the services inside the different point of distribution grid. This methodology, using the statistical mobility data of Niort, a city in west of France, was applied and possible services for this city were identified.

This study showed that based on the actual provision of PEV evolution in France, the services peak power shaving in MV grid, frequency regulation, losses minimization and energy transmission cost minimization are more competitive compared to balancing mechanism, voltage regulation and peak power shaving in LV grid. It should be taken into account that, the impact of V2G infrastructure development and availability of V2G per individual vehicle are also another important factor that may affect the presented results. The general approach presented in this paper is sufficiently discussed, and it has potential to be applied on other similar case studies.

12. Acknowledgement

The authors kindly acknowledge the financial supports of ADEME (French Environment and Energy Management Agency), GEREDIS Deux-sèvres (Deux-sèvres Department Distribution System Operator (DSO)), SEOLIS (Energy supplier of department Deux-sèvres) and SNCF (French National Railway Network) for this project and also GEREDIS Deux-sèvres for their support of information for local distribution grid and INSEE (French National Institute of Statistics and Economic Studies) for the regional mobility and traffic survey information.

References

[1] K. Clement-Nyns, E. Haesen, J. Driesen, The impact of charging plug-in hybrid electric vehicles on a residential distribution grid, IEEE Transactions on Power Systems 25 (1) (2010) 371–380. doi:10.1109/TPWRS.2009.2036481.

[2] K. Clement-Nyns, E. Haesen, J. Driesen, The impact of vehicle-to-grid on the distribution grid, Electric Power Systems Research 81 (1) (2011) 185 – 192. doi:http://dx.doi.org/10.1016/j.epsr.2010.08.007.

[3] S. Sarabi, A. Davigny, V. Courtecuisse, Y. Riffonneau, B. Robyns, Traffic-based modeling of electric vehicle charging load and its impact on the distribution network and railway station parking lots, in: 2014 3rd International Symposium on Environmental Friendly Energies and Applications (EFEA), 2014, pp. 1–6. doi:10.1109/EFEA.2014.7059977.

[4] Z. Xu, Z. Hu, Y. Song, W. Zhao, Y. Zhang, Coordination of PEVs charging across multiple aggregators, Applied Energy 136 (2014) 582 – 589. doi:http://dx.doi.org/10.1016/j.apenergy.2014.08.116.

[5] E. Sortomme, M. Hindi, S. MacPherson, S. Venkata, Coordinated charging of plug-in hybrid electric vehicles to minimize distribution system losses, IEEE Transactions on Smart Grid 2 (1) (2011) 198–205. doi:10.1109/TSG.2010.2090913.

[6] J. Hu, S. You, M. Lind, J. Ostergaard, Coordinated charging of electric vehicles for congestion prevention in the distribution grid, IEEE Transactions on Smart Grid 5 (2) (2014) 703–711. doi:10.1109/TSG.2013.2279007.

[7] J. Yang, L. He, S. Fu, An improved PSO-based charging strategy of electric vehicles in electrical distribution grid, Applied Energy 128 (2014) 82 – 92. doi:http://dx.doi.org/10.1016/j.apenergy.2014.04.047.

[8] J. Tomi, W. Kempton, Using fleets of electric-drive vehicles for grid support, Journal of Power Sources 168 (2) (2007) 459 – 468. doi:http://dx.doi.org/10.1016/j.jpowsour.2007.03.010.

[9] W. Kempton, J. Tomi, Vehicle-to-grid power implementation: From stabilizing the grid to supporting large-scale renewable energy, Journal of Power Sources 144 (1) (2005) 280 – 294. doi:http://dx.doi.org/10.1016/j.jpowsour.2004.12.022.

[10] Z. Luo, Z. Hu, Y. Song, Z. Xu, H. Liu, L. Jia, H. Lu, Economic analyses of plug-in electric vehicle battery providing ancillary services, in: Electric Vehicle Conference (IEVC), 2012 IEEE International, 2012, pp. 1–5. doi:10.1109/IEVC.2012.6183272.

[11] A. De Los Rios, J. Goentzel, K. Nordstrom, C. Siegert, Economic analysis of vehicle-to-grid (V2G)-enabled fleets participating in the regulation service market, in: Innovative Smart Grid Technologies (ISGT), 2012 IEEE PES, 2012, pp. 1–8. doi:10.1109/ISGT.2012.6175658.

[12] S. Han, S. Han, K. Sezaki, Economic assessment on V2G frequency regulation regarding the battery degradation, in: Innovative Smart Grid Technologies (ISGT), 2012 IEEE PES, 2012, pp. 1–6. doi:10.1109/ISGT.2012.6175717.

[13] Y. Gao, Y. Chen, C.-Y. Wang, K. Liu, A contract-based approach for ancillary services in V2G networks: Optimality and learning, in: INFOCOM, 2013 Proceedings IEEE, 2013, pp. 1151–1159. doi:10.1109/INFCOM.2013.6566906.

[14] M. Ehsani, M. Falahi, S. Lotfifard, Vehicle to grid services: Potential and applications, Energies 5 (10) (2012) 4076. doi:10.3390/en5104076.

[15] S. Han, S. Han, K. Sezaki, Estimation of Achievable Power Capacity From Plug-in Electric Vehicles for V2G Frequency Regulation: Case Studies for Market Participation, IEEE Transactions on Smart Grid 2 (4) (2011) 632–641. doi:10.1109/TSG.2011.2160299.

[16] I. Pavi, T. Capuder, I. Kuzle, Value of flexible electric vehicles in providing spinning reserve services, Applied Energy 157 (2015) 60–74. doi:10.1016/j.apenergy.2015.07.070.

[17] L. Jian, Y. Zheng, X. Xiao, C. C. Chan, Optimal scheduling for vehicle-to-grid operation with stochastic connection of plug-in electric vehicles to smart grid, Applied Energy 146 (2015) 150–161. doi:10.1016/j.apenergy.2015.02.030.

[18] M. Falahi, H.-M. Chou, M. Ehsani, L. Xie, K. Butler-Purry, Potential Power Quality Benefits of Electric Vehicles, IEEE Transactions on Sustainable Energy 4 (4) (2013) 1016–1023. doi:10.1109/TSTE.2013.2263848.

[19] C. Quinn, D. Zimmerle, T. H. Bradley, The effect of communication architecture on the availability, reliability, and economics of plug-in hybrid electric vehicle-to-grid ancillary services, Journal of Power Sources 195 (5) (2010) 1500–1509. doi:10.1016/j.jpowsour.2009.08.075.

[20] J. D. K. Bishop, C. J. Axon, D. Bonilla, M. Tran, D. Banister, M. D. McCulloch, Evaluating the impact of V2G services on the degradation of batteries in PHEV and EV, Applied Energy 111 (2013) 206–218. doi:10.1016/j.apenergy.2013.04.094.

[21] H. Khayyam, A. Bab-Hadiashar, Adaptive intelligent energy management system of plug-in hybrid electric vehicle, Energy 69 (2014) 319 – 335. doi:http://dx.doi.org/10.1016/j.energy.2014.03.020.

[22] H. Khayyam, J. Abawajy, B. Javadi, A. Goscinski, A. Stojcevski, A. Bab-Hadiashar, Intelligent battery energy management and control for vehicle-to-grid via cloud computing network, Applied Energy 111 (2013) 971 – 981. doi:http://dx.doi.org/10.1016/j.apenergy.2013.06.021.

[23] H. Khayyam, H. Ranjbarzadeh, V. Marano, Intelligent control of vehicle to grid power, Journal of Power Sources 201 (2012) 1 – 9. doi:http://dx.doi.org/10.1016/j.jpowsour.2011.11.010.

[24] M. WANG, Y. MU, H. JIA, J. WU, X. YAO, X. YU, J. EKANAYAKE, A preventive control strategy for static voltage stability based on an efficient power plant model of electric vehicles, Journal of Modern Power Systems and Clean Energy 3 (1) (2015) 103–113. doi:10.1007/s40565-014-0092-9.

[25] M. Wang, P. Zeng, Y. Mu, H. Jia, W. Liang, Y. Qi, An efficient power plant model of electric vehicles considering the travel behaviors of ev users, in: Power System Technology (POWERCON), 2014 International Conference on, 2014, pp. 3322–3327. doi:10.1109/POWERCON.2014.6993890.

[26] French Transmission System Operator, RTE (2014).
URL https://clients.rte-france.com/lang/fr/visiteurs/services/actualites.jsp?id=9693&mode=detail

[27] G. Delille, B. Francois, G. Malarange, J.-L. Fraisse, Energy storage systems in distribution grids: new assets to upgrade distribution networks abilities, in: Proc. 20th International Conference and Exhibition on Electricity Distribution (CIRED2009), 2009, pp. 18–19. doi:10.1049/cp.2009.0790.

[28] J. Fluhr, K.-H. Ahlert, C. Weinhardt, A Stochastic Model for Simulating the Availability of Electric Vehicles for Services to the Power Grid, in: 2010 43rd Hawaii International Conference on System Sciences (HICSS), 2010, pp. 1–10. doi:10.1109/HICSS.2010.33.

[29] F. Soares, J. Peas Lopes, P. Rocha Almeida, C. Moreira, L. Seca, A stochastic model to simulate electric vehicles motion and quantify the energy required from the grid, in: 17th Power Systems Computation Conference, Stockholm, 2011, pp. 1–7.
URL http://www.pscc-central.org/uploads/tx_ethpublications/fp359.pdf

[30] J. Rolink, C. Rehtanz, Large-Scale Modeling of Grid-Connected Electric Vehicles, IEEE Transactions on Power Delivery 28 (2) (2013) 894–902. doi:10.1109/TPWRD.2012.2236364.

[31] M. Gonzalez Vaya, G. Andersson, S. Boyd, Decentralized control of plug-in electric vehicles under driving uncertainty, in: Innovative Smart Grid Technologies Conference Europe (ISGT-Europe), 2014 IEEE PES, 2014, pp. 1–6. doi:10.1109/ISGTEurope.2014.7028989.

[32] L. Agarwal, W. Peng, L. Goel, Probabilistic estimation of aggregated power capacity of EVs for vehicle-to-grid application, in: 2014 International Conference on Probabilistic Methods Applied to Power Systems (PMAPS), 2014, pp. 1–6. doi:10.1109/PMAPS.2014.6960592.

[33] J. Mathieu, M. Gonzalez Vaya, G. Andersson, Uncertainty in the flexibility of aggregations of demand response resources, in: IECON 2013 - 39th Annual Conference of the IEEE Industrial Electronics Society, 2013, pp. 8052–8057. doi:10.1109/IECON.2013.6700479.

[34] M. G. Vay, G. Andersson, Smart Charging of Plug-in Electric Vehicles Under Driving Behavior Uncertainty, in: R. Karki, R. Billinton, A. K. Verma (Eds.), Reliability Modeling and Analysis of Smart Power Systems, Reliable and Sustainable Electric Power and Energy Systems Management, Springer India, 2014, pp. 85–99. doi:10.1007/978-81-322-1798-5_6.

[35] I. Momber, A. Siddiqui, T. Gomez San Roman, L. Soder, Risk Averse Scheduling by a PEV Aggregator Under Uncertainty, IEEE Transactions on Power Systems 30 (2) (2015) 882–891. doi:10.1109/TPWRS.2014.2330375.

[36] Home-work migration statistics in Poitou-Charentes region, INSEE (2010).
URL http://www.iaat.org/outils/statistiques/index.php?site=IAAT&fichier=1355

[37] S. Sarabi, L. Kefsi, A. Merdassi, B. Robyns, Supervision of plug-in electric vehicles connected to the electric distribution grids, International Journal of Electrical Energy 1 (4) (2013) 256–263. doi:10.12720/ijoee.1.4.256-263.

[38] S. Sarabi, A. Davigny, Y. Riffonneau, V. Courtecuisse, B. Robyns, Contribution and impacts of grid integrated electric vehicles to the distribution networks and railway station parking lots, in: Electricity Distribution (CIRED 2015), 23rd International Conference and Exhibition on, 2015, pp. 1–5.
URL http://cired.net/publications/cired2015/papers/CIRED2015_1505_final.pdf

[39] F. Salah, J. P. Ilg, C. M. Flath, H. Basse, C. v. Dinther, Impact of electric vehicles on distribution substations: A Swiss case study, Applied Energy 137 (2015) 88–96. doi:10.1016/j.apenergy.2014.09.091.

[40] Daily travel survey in Niort, INSEE Poitou-Charentes (2003). URL http://www.agglo-niort.fr/pdu/IMG/pdf/EnqueteMenageNiort3.pdf

[41] C. Zhou, K. Qian, M. Allan, W. Zhou, Modeling of the cost of ev battery wear due to V2G application in power systems, IEEE Transactions on Energy Conversion 26 (4) (2011) 1041–1050. doi:10.1109/TEC.2011.2159977.

[42] S. Gill, B. Stephen, S. Galloway, Wind turbine condition assessment through power curve copula modeling, IEEE Transactions on Sustainable Energy 3 (1) (2012) 94–101. doi:10.1109/TSTE.2011.2167164.

[43] E. Pashajavid, M. Golkar, Non-Gaussian multivariate modeling of plug-in electric vehicles load demand, International Journal of Electrical Power and Energy Systems 61 (2014) 197 – 207. doi:http://dx.doi.org/10.1016/j.ijepes.2014.03.021.

[44] S. Demarta, A. J. McNeil, The t copula and related copulas, International statistical review 73 (1) (2005) 111–129.

[45] G. McLachlan, D. Peel, Finite mixture models, John Wiley & Sons, 2004.

[46] L. Wen, L. Gao, X. Li, L. Zhang, Free Pattern Search for global optimization, Applied Soft Computing 13 (9) (2013) 3853 – 3863. doi:http://dx.doi.org/10.1016/j.asoc.2013.05.004.

[47] S. Sarabi, A. Bouallaga, A. Davigny, B. Robyns, V. Courtecuisse, Y. Riffonneau, M. Regner, The feasibility of the ancillary services for vehicle-to-grid technology, in: European Energy Market (EEM), 2014 11th International Conference on the, 2014, pp. 1–5. doi:10.1109/EEM.2014.6861251.

[48] B. Robyns, B. François, G. Delille, C. Saudemont, Applications and values of energy storage in power systems, in: Energy Storage in Electric Power Grids, Wiley Online Library, 2015, pp. 55–152. doi:10.1002/9781119058724.ch3.

[49] M. Azzouz, M. Shaaban, E. El-Saadany, Real-time optimal voltage regulation for distribution networks incorporating high penetration of PEVs, IEEE Transactions on Power Systems 30 (6) (2015) 3234–3245. doi:10.1109/TPWRS.2014.2385834.

[50] P. Codani, M. Petit, Y. Perez, Participation of an electric vehicle fleet to primary frequency control in France, International Journal of Electric and Hybrid Vehicles 7 (3) (2015) 233–249. doi:10.1504/IJEHV.2015.071639.